

Solvable Critical Dense Polymers on the Cylinder

Paul A. Pearce, Jørgen Rasmussen, Simon P. Villani

*Department of Mathematics and Statistics, University of Melbourne
Parkville, Victoria 3010, Australia*

P.Pearce@ms.unimelb.edu.au, J.Rasmussen@ms.unimelb.edu.au
S.Villani@ms.unimelb.edu.au

Abstract

A lattice model of critical dense polymers is solved exactly on a cylinder with finite circumference. The model is the first member $\mathcal{LM}(1,2)$ of the Yang-Baxter integrable series of logarithmic minimal models. The cylinder topology allows for non-contractible loops with fugacity α that wind around the cylinder or for an arbitrary number ℓ of defects that propagate along the full length of the cylinder. Using an enlarged periodic Temperley-Lieb algebra, we set up commuting transfer matrices acting on states whose links are considered distinct with respect to connectivity around the front or back of the cylinder. These transfer matrices satisfy a functional equation in the form of an inversion identity. For even N , this involves a non-diagonalizable braid operator \mathbf{J} and an involution $\mathbf{R} = -(\mathbf{J}^3 - 12\mathbf{J})/16 = (-1)^{\mathbf{F}}$ with eigenvalues $R = (-1)^{\ell/2}$. This is reminiscent of supersymmetry with a pair of defects interpreted as a fermion. The number of defects ℓ thus separates the theory into Ramond ($\ell/2$ even), Neveu-Schwarz ($\ell/2$ odd) and \mathbb{Z}_4 (ℓ odd) sectors. For the case of loop fugacity $\alpha = 2$, the inversion identity is solved exactly sector by sector for the eigenvalues in finite geometry. The eigenvalues are classified by the physical combinatorics of the patterns of zeros in the complex spectral-parameter plane. This yields selection rules for the physically relevant solutions to the inversion identity. The finite-size corrections are obtained from Euler-Maclaurin formulas. In the scaling limit, we obtain the conformal partition functions as sesquilinear forms and confirm the central charge $c = -2$ and conformal weights $\Delta, \bar{\Delta} = \Delta_t = (t^2 - 1)/8$. Here $t = \ell/2$ and $t = 2r - s \in \mathbb{N}$ in the ℓ even sectors with Kac labels $r = 1, 2, 3, \dots; s = 1, 2$ while $t \in \mathbb{Z} - \frac{1}{2}$ in the ℓ odd sectors. Strikingly, the $\ell/2$ odd sectors exhibit a \mathcal{W} -extended symmetry but the $\ell/2$ even sectors do not. Moreover, the naive trace summing over all ℓ even sectors does not yield a modular invariant.

Contents

1	Introduction	2
2	Lattice Model	3
2.1	Critical dense polymers	3
2.2	Cylinder Temperley-Lieb algebra	4
2.3	Periodic Temperley-Lieb algebra and its enlargement	5
3	Cylinder Transfer Matrix	6
3.1	Single-row transfer matrix	6
3.2	Hamiltonian limit	7
3.3	Link states	7
3.4	Augmented link states	8
4	Inversion Identities	10
4.1	Cylinder inversion identity	10
4.2	Matrix realization of \mathbf{J}	11
4.3	Braid limits	12
4.4	Matrix inversion identities	12
4.5	Identified connectivities	13
5	Solution on a Finite Cylinder	13
5.1	Finite-size corrections	14
5.2	\mathbb{Z}_4 sectors (N odd, ℓ odd)	15
5.3	Ramond and Neveu-Schwarz sectors (N even, ℓ even)	18
6	Finite-Size Corrections from Euler-Maclaurin	24
7	Physical Combinatorics and Selection Rules	25
7.1	\mathbb{Z}_4 sectors (N odd, ℓ odd)	25
7.2	Ramond sectors (N even, $\ell/2$ even)	28
7.3	Neveu-Schwarz sectors (N even, $\ell/2$ odd)	30
7.4	Finitized characters in Ramond and Neveu-Schwarz sectors	32
8	Conformal Partition Functions	34
9	Conclusion	36
A	Properties of \mathbf{J}	37
A.1	Proof of Inversion Identity	37
A.2	Proof of Drop-Down Lemma	38
A.3	Proof of Sector Lemma	39
A.4	Matrix \mathbf{J} for an arbitrary number of defects	39

1 Introduction

Familiar materials such as plastics, nylon, polyester and plexiglass are made from polymers. Polymers [1] consist of very long chain molecules with a large number of repeating structural units called monomers. Polymers exist in low- or high-temperature phases which are characterised as either dense or dilute. Polymers are *dense* if they fill a finite (non-zero) fraction of the available volume in the thermodynamic limit.

The modern era of two-dimensional polymer theory began in the late eighties [2, 3, 4] when Saleur and Duplantier initiated the study of polymers as a conformal field theory (CFT). From the viewpoint of lattice statistical mechanics, polymers are of interest as a prototypical example of a system involving (extended) non-local degrees of freedom. It might be expected that the non-local nature of these degrees of freedom has a profound effect on the associated CFT obtained in the continuum scaling limit. Indeed, the associated CFT is in fact *logarithmic* [5] in the sense that, for certain representations, the Virasoro dilatation generator L_0 is non-diagonalizable and exhibits non-trivial 2×2 Jordan blocks.

In this paper, we consider a Yang-Baxter integrable model of critical dense polymers on a cylinder, both on the lattice and in the continuum scaling limit. In fact, this model is the first member $\mathcal{LM}(1, 2)$ of the infinite series of logarithmic minimal models $\mathcal{LM}(p, p')$ [6]. An alternative approach to logarithmic CFT based on quantum spin chains appears in [7]. The fugacity of contractible loops for $\mathcal{LM}(1, 2)$ is $\beta = 0$. Previously [8], we considered this model on finite-width strips with various boundary conditions. The associated integrals of motion and Baxter's Q matrix have been considered in [9]. The solvable critical dense polymer model on a *cylinder* is built from a (locally) planar version [10] of the periodic Temperley-Lieb algebra [11]. Because of the non-local degrees of freedom, logarithmic theories are sensitive to the topology. So changing the topology from a strip to a cylinder has profound effects. Specifically, a cylinder topology allows for non-contractible loops with fugacity α that wind around the cylinder or for defects that propagate along the full length of the cylinder. These can have dramatic effects on the properties of the model. The number of defects ℓ is a quantum number that separates the theory into Ramond ($\ell/2$ even), Neveu-Schwarz ($\ell/2$ odd) and \mathbb{Z}_4 (ℓ odd) sectors. Following [4, 12], we use the terminology of supersymmetry even though we do not claim any superconformal symmetry in our model.

Remarkably, as for the square lattice Ising model [13], the commuting single-row transfer matrices of this model satisfy a simple functional equation in the form of an inversion identity. This enables us to solve for the exact eigenvalues of the transfer matrices on a finite lattice for $\alpha = 2$. The conformal spectra are readily accessible from finite-size corrections. In particular, in the continuum scaling limit, we obtain the partition functions as sesquilinear forms and confirm the central charge $c = -2$ and conformal weights $\Delta, \bar{\Delta} = \Delta_t = (t^2 - 1)/8$. Here $t = \ell/2$ and $t = 2r - s \in \mathbb{N}$ in the ℓ even sectors with Kac labels $r = 1, 2, 3, \dots; s = 1, 2$ while $t \in \mathbb{Z} - \frac{1}{2}$ in the ℓ odd sectors. On the strip, this model admits a \mathcal{W} -extended conformal algebra and is identified [14] with *symplectic fermions* [15]. Strikingly, on the cylinder, we find that this extended symmetry only holds in the sum over $\ell/2$ odd sectors and not in the sum over $\ell/2$ even sectors. Moreover, the naive trace summing over all even N sectors does not yield the known modular invariant [16] of the $c_{1,2}$ triplet model.

The layout of this paper is as follows. In Section 2, we define the solvable critical dense polymer lattice model. We also discuss the periodic Temperley-Lieb (TL) algebra, its enlargement by adding the shift operators Ω and Ω^{-1} , and its relation to the *cylinder* TL

algebra which is a direct generalization of the planar TL algebra of Jones [10]. In Section 3, we define the single-row transfer matrices directly in the cylinder TL algebra. We also define the vector spaces of link states on which these transfer matrices act and relate these to the cases of *distinct* (DC) and *identified* (IC) connectivities [17]. The inversion identities are derived in Section 4, first in the setting of the cylinder TL algebra and then as matrix inversion identities. Certain details are deferred to Appendix A. The inversion identities are solved sector by sector for the transfer matrix eigenvalues in Section 5, while the finite-size corrections are extracted in Section 6. In Section 7, the physically relevant solutions are obtained empirically and encoded by applying physical combinatorics supplemented by selection rules. Finitized conformal partition functions are obtained as sesquilinear forms in finitized characters [18]. The conformal partition functions arising in the continuum scaling limit are discussed in Section 8. We conclude with some remarks and directions for future research in Section 9.

2 Lattice Model

2.1 Critical dense polymers

To model critical dense polymers on a cylinder with a finite circumference, we consider a square lattice on a strip, with N columns and M rows of faces, and identify the left and right edges as shown in Figure 1.

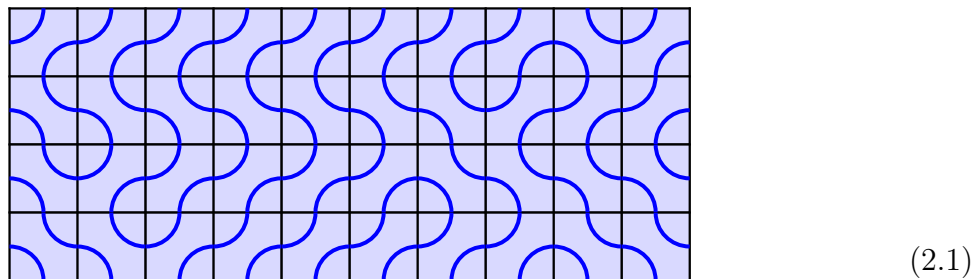


Figure 1: A typical dense polymer configuration on a 10×4 cylindrical lattice. The left and right edges are identified to form a cylinder. In this case, the circumference is $N = 10$ and $M = 4$. No local closed loops are formed on the surface of the cylinder in accord with the vanishing loop fugacity $\beta = 0$. It is, however, possible to allow non-contractible loops encircling the cylinder with fugacity $\alpha \neq 0$.

An elementary face of the lattice can assume one of two configurations with different statistical weights

$$\begin{array}{|c|} \hline \text{or} \\ \hline \end{array}
 \begin{array}{c}
 \begin{array}{|c|} \hline \text{or} \\ \hline \end{array}
 \end{array}
 \quad \text{or} \quad
 \begin{array}{c}
 \begin{array}{|c|} \hline \text{or} \\ \hline \end{array}
 \end{array}
 \quad (2.2)$$

where the arcs represent local segments of polymers. The two possible configurations can be combined into a single face operator as

$$X(u) = \begin{array}{|c|} \hline u \\ \hline \end{array} = \cos u \begin{array}{|c|} \hline \text{or} \\ \hline \end{array} + \sin u \begin{array}{|c|} \hline \text{or} \\ \hline \end{array} \quad (2.3)$$

where u is the *spectral parameter* related to spatial anisotropy. The lower left corner is marked to fix the orientation of the square.

Since the polymer segments pass uniformly through each face, this is a model of *dense* polymers — in the continuum scaling limit, a polymer is space-filling and has fractal dimension 2. The non-local degrees of freedom correspond to a number of polymers. It is often convenient to think of these degrees of freedom as non-local connectivities.

Critical dense polymers corresponds to the first member $\mathcal{LM}(1, 2)$ of the infinite series $\mathcal{LM}(p, p')$ of logarithmic minimal models [6]. Each logarithmic model is characterized by a crossing parameter $\lambda = \frac{p'-p}{p'}\pi$ related to the loop fugacity β by

$$\beta = 2 \cos \lambda = 2 \cos \frac{p' - p}{p'} \pi, \quad p, p' \text{ coprime} \quad (2.4)$$

It was argued in [6] that the scaling limits of these integrable lattice models yield logarithmic CFTs. In the case of critical dense polymers,

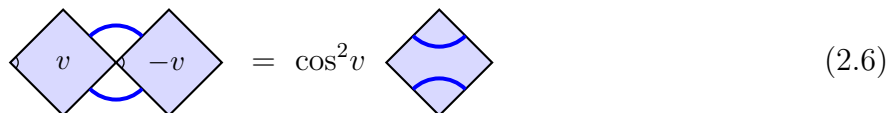
$$\lambda = \frac{\pi}{2}, \quad \beta = 0 \quad (2.5)$$

implying that local contractible loops are not allowed.

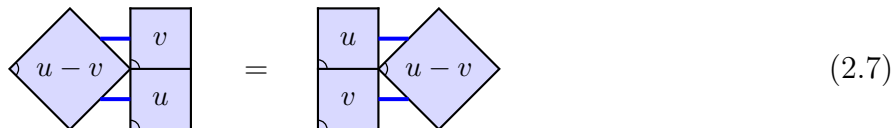
2.2 Cylinder Temperley-Lieb algebra

For the purposes of this paper, the *cylinder* Temperley-Lieb (TL) algebra is a diagrammatic algebra built up from elementary faces. The faces are connected such that the midpoint of an outer edge of a face, called a node, can be linked to a node of any other (or even the same) face as long as the total set of links make up a *non-intersecting* web of connections on the surface of a cylinder. The cylinder TL algebra is equivalent to the annular algebra of Jones [10].

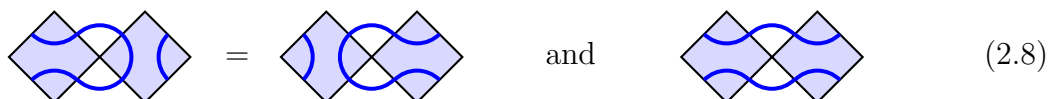
Two basic local properties of the cylinder TL algebra are the inversion relation



and the Yang-Baxter equation (YBE) [13]



These are identities for 2- and 3-tangles, respectively, where a k -tangle is an arrangement of faces with $2k$ free nodes. The identities are established by writing out all the possible configurations, while keeping track of the associated weights, and collecting them in classes according to connectivities. The left side of (2.6), for example, thus corresponds to a sum of four terms of which one vanishes since $\beta = 0$. The remaining three terms fall into the two connectivity classes



The weights accompanying the two equivalent configurations cancel since $\cos v \sin(-v) + \sin v \cos(-v) = 0$, while the last diagram comes with the weight $\cos v \cos(-v)$ thereby yielding the identity (2.6).

Particular elements of the cylinder TL algebra are the *shift* or *winding* operator Ω and its inverse Ω^{-1}

$$\Omega = \begin{array}{|c|c|c|c|c|c|c|c|c|c|} \hline \text{Diagram of } \Omega \text{ (shift operator)} \\ \hline \end{array} \quad (2.9)$$

$$\Omega^{-1} = \begin{array}{|c|c|c|c|c|c|c|c|c|c|} \hline \text{Diagram of } \Omega^{-1} \text{ (inverse shift operator)} \\ \hline \end{array} \quad (2.10)$$

The multiplication implied in

$$\Omega \Omega^{-1} = \Omega^{-1} \Omega = \mathbf{I} \quad (2.11)$$

is vertical concatenation, and \mathbf{I} is the (vertical) identity operator linking every node on the upper horizontal edge to the node directly below it on the lower horizontal edge.

2.3 Periodic Temperley-Lieb algebra and its enlargement

The *periodic* (affine) TL algebra [11] of size N is generated by the identity I and the generators e_j

$$\mathcal{TL}(N) = \langle I, e_0, e_1, \dots, e_{N-1} \rangle \quad (2.12)$$

subject to the periodicity constraints

$$e_j \equiv e_{j \bmod N}, \quad j \in \mathbb{Z} \quad (2.13)$$

and the relations

$$e_j^2 = \beta e_j, \quad e_j e_{j \pm 1} e_j = e_j, \quad j = 0, 1, \dots, N-1 \quad (2.14)$$

$$e_j e_k = e_k e_j, \quad j - k \neq 0, \pm 1 \bmod N \quad (2.15)$$

where β is the fugacity of contractible loops. The TL generators e_j are represented diagrammatically by monoids [20]. The face operator at position j is given by

$$X_j(u) = \cos u I + \sin u e_j \quad (2.16)$$

and obtained by rotating the face operator in (2.3) by 45 degrees in the counter-clockwise direction. The periodic TL algebra is infinite dimensional.

For N even, one introduces the combinations

$$E = e_0 e_2 e_4 \cdots e_{N-2}, \quad F = e_1 e_3 e_5 \cdots e_{N-1}, \quad E^2 = \beta^{\frac{N}{2}} E, \quad F^2 = \beta^{\frac{N}{2}} F \quad (2.17)$$

Letting α denote the fugacity of *non-contractible* loops, these can be ‘removed’ in pairs

$$EFE = \alpha^2 E, \quad FEF = \alpha^2 F \quad (2.18)$$

For N odd, non-contractible loops cannot appear.

The elements Ω and Ω^{-1} (2.10) of the cylinder TL algebra are *not* elements of the periodic TL algebra. They may be included [19], though, thereby enlarging the periodic TL algebra. Translation on the TL generators is then implemented by conjugation

$$e_{j-1} = \Omega e_j \Omega^{-1} \quad (2.19)$$

so that the enlarged TL algebra is generated by three independent generators

$$\mathcal{ETL}(N) = \langle e_0, \Omega, \Omega^{-1} \rangle \quad (2.20)$$

The periodicity constraints (2.13) and the relations (2.14) and (2.15) now read

$$\Omega^N e_0 \Omega^{-N} = e_0 \quad (2.21)$$

$$e_0^2 = \beta e_0, \quad e_0 \Omega^{\mp 1} e_0 \Omega^{\pm 1} e_0 = e_0 \quad (2.22)$$

$$e_0 \Omega^j e_0 \Omega^{-j} = \Omega^j e_0 \Omega^{-j} e_0, \quad j = 2, \dots, N-2 \quad (2.23)$$

For N even, we furthermore have

$$E = (e_0 \Omega^{-2})^{\frac{N}{2}} \Omega^N = \Omega^{-N} (\Omega^2 e_0)^{\frac{N}{2}} \quad (2.24)$$

$$F = \Omega^{-1} (e_0 \Omega^{-2})^{\frac{N}{2}} \Omega^{N+1} = \Omega^{-N-1} (\Omega^2 e_0)^{\frac{N}{2}} \Omega \quad (2.25)$$

$$E = \Omega F \Omega^{-1}, \quad F = \Omega^{-1} E \Omega \quad (2.26)$$

and

$$E \Omega^{\pm 1} E = \alpha E, \quad F \Omega^{\pm 1} F = \alpha F \quad (2.27)$$

indicating that non-contractible loops can now be removed one by one.

3 Cylinder Transfer Matrix

3.1 Single-row transfer matrix

Having introduced the cylinder TL algebra, we now define diagrammatically the single-row N -tangle

$$\mathbf{T}(u) = \begin{array}{c} \begin{array}{|c|c|c|c|c|c|c|c|} \hline u & & \dots & & & & \dots & & u \\ \hline \end{array} \\ \hline \end{array} \quad (3.1)$$

consisting of N faces where the dependence on N is suppressed. The left and right edges are identified in accord with the periodicity of the cylinder. As discussed below, $\mathbf{T}(u)$ has a natural matrix representation when acting vertically from below on a given set of periodic link states. We thus refer to it as the (single-row) “transfer matrix”, even though it is defined as a cylinder N -tangle without reference to any matrix representation. The shift operator Ω and its inverse Ω^{-1} enter naturally as the limits

$$\lim_{u \rightarrow 0} \mathbf{T}(u) = \Omega, \quad \lim_{u \rightarrow \lambda} \mathbf{T}(u) = \Omega^{-1} \quad (3.2)$$

Using standard diagrammatic arguments [13], it follows that $\mathbf{T}(u)$ gives rise to a commuting family of transfer matrices where

$$[\mathbf{T}(u), \mathbf{T}(v)] = 0 \quad (3.3)$$

As in (2.11), the implied multiplication in the commutator means vertical concatenation of the two N -tangles in the cylinder TL algebra. It follows, in particular, that $[\mathbf{T}(u), \Omega^{\pm 1}] = 0$.

3.2 Hamiltonian limit

The Hamiltonian limit of the transfer matrix $\mathbf{T}(u)$ is defined in the cylinder TL algebra as the N -tangle appearing as the first sub-leading term in an expansion with respect to u . We define \mathbf{H} as this N -tangle up to a factor of Ω , that is,

$$\mathbf{T}(u) = \Omega[\mathbf{I} - u\mathbf{H} + O(u^2)] \quad (3.4)$$

where \mathbf{I} is the vertical identity diagram

$$\mathbf{I} = \begin{array}{|c|c|c|c|c|} \hline \color{blue}{|} & \color{blue}{|} & \color{blue}{|} & \dots & \color{blue}{|} \\ \hline \end{array} \quad (3.5)$$

It follows that

$$-\mathbf{H} = \begin{array}{|c|c|c|c|c|} \hline \color{blue}{\cup} & \color{blue}{|} & \color{blue}{|} & \dots & \color{blue}{|} \\ \color{blue}{\cup} & \color{blue}{|} & \color{blue}{|} & \dots & \color{blue}{|} \\ \hline \end{array} + \begin{array}{|c|c|c|c|c|} \hline \color{blue}{\cup} & \color{blue}{|} & \color{blue}{|} & \dots & \color{blue}{|} \\ \color{blue}{\cup} & \color{blue}{|} & \color{blue}{|} & \dots & \color{blue}{|} \\ \hline \end{array} + \dots + \begin{array}{|c|c|c|c|c|} \hline \color{blue}{\cup} & \color{blue}{|} & \color{blue}{|} & \dots & \color{blue}{|} \\ \color{blue}{\cup} & \color{blue}{|} & \color{blue}{|} & \dots & \color{blue}{|} \\ \hline \end{array} \quad (3.6)$$

which in terms of the generators of the *periodic* TL algebra merely corresponds to

$$\mathbf{H} = - \sum_{j=0}^{N-1} e_j \quad (3.7)$$

3.3 Link states

A matrix representation of $\mathbf{T}(u)$ is obtained by acting with $\mathbf{T}(u)$ from below on a suitable vector space of link states. Suppose there are N nodes arranged periodically around the upper horizontal edge of the cylinder. For N even, a link state specifies how these N nodes are linked together. Two nodes can be connected by the front of the cylinder or by the back. We can consider these two connections as *distinct* or we can choose to *identify* the two connections and their corresponding link states. In the latter case, we can think of a hemi-spherical cap placed on the top of the cylinder so that a connection by the back of the cylinder can be continuously deformed to a connection by the front and vice versa. The link states are locally planar in the sense that connections are not allowed to cross on the extended surface of the cylinder (or capped cylinder).

The enlarged TL algebra is the appropriate algebra when acting on link states with *distinct connectivities* (DC). In the topology associated with the action on link states with *identified connectivities* (IC), all loops become contractible. This implies that the appropriate algebra in this case is the enlarged TL algebra with $\alpha = \beta$. In either case, the enlarged TL

algebra is effectively finite when acting on the (DC or IC) link states since the corresponding matrix realizations satisfy

$$\Omega^N = (\Omega^{-1})^N = I \quad (3.8)$$

This means that we do not keep track of windings around the cylinder. As matrices, the inverse shift operator is given by the Hermitian conjugate of the operator itself

$$\Omega^{-1} = \Omega^\dagger \quad (3.9)$$

For $N = 4$, there are six DC link states



$$\quad (3.10)$$

and two IC link states



$$\quad (3.11)$$

In general, the dimension of the vector space of link states for DC and IC is given by the central binomial coefficients and Catalan numbers

$$\dim(V_N^{\text{DC}}) = \binom{2n}{n}, \quad \dim(V_N^{\text{IC}}) = \frac{1}{n+1} \binom{2n}{n}, \quad n = \frac{N}{2}, \quad N \text{ even} \quad (3.12)$$

A node that is not linked to another node gives rise to a *defect* which may be viewed as a link to the point (above) at infinity. For N odd, there is at least one defect. In the presence of defects, there is only one way (either by the front or by the back) to connect two nodes, so there is no distinction between identified and distinct connectivities. The dimension of the space of link states with precisely ℓ defects is

$$\dim(V_N^{(\ell)}) = \binom{N}{\frac{N-\ell}{2}}, \quad \ell = N \bmod 2 \quad (3.13)$$

It is the set of DC link states which corresponds to this for $\ell = 0$: $V_N^{(0)} = V_N^{\text{DC}}$. For $N = 3$ and $\ell = 1$, there are 3 link states



$$\quad (3.14)$$

We note that (3.8) and (3.9) remain valid when acting on link states with defects. Also, defects can be annihilated in pairs, but not created, by the action of the cylinder TL algebra. If we allow for an *arbitrary* number of defects of given parity, the number of link states is

$$\sum_{\ell \in 2\mathbb{N}-1} \binom{N}{\frac{N-\ell}{2}} = 2^{N-1}, \quad \sum_{\ell \in 2\mathbb{N}_0} \binom{N}{\frac{N-\ell}{2}} = 2^{N-1} - \frac{1}{2} \binom{N}{\frac{N}{2}} \quad (3.15)$$

3.4 Augmented link states

When the direction of transfer is fixed, the cylinder TL algebra reduces to the enlarged (periodic) TL algebra. The transfer N -tangle then acts naturally on link states with N nodes. For the purpose of computer calculations, however, the transfer matrix is conveniently

written in terms of the enlarged TL algebra $\mathcal{ETL}(N + 2)$ acting on a suitable vector space of link states of size $N + 2$. Explicitly,

$$\mathbf{T}(u) = e_N \prod_{j=-1}^{N-2} X_j(u) \Omega \quad (3.16)$$

as shown in Figure 2, where the face operators are given by (2.16). The link states are all augmented by a spectator half-arc joining the nodes in positions N and $N + 1$. For $N = 4$,

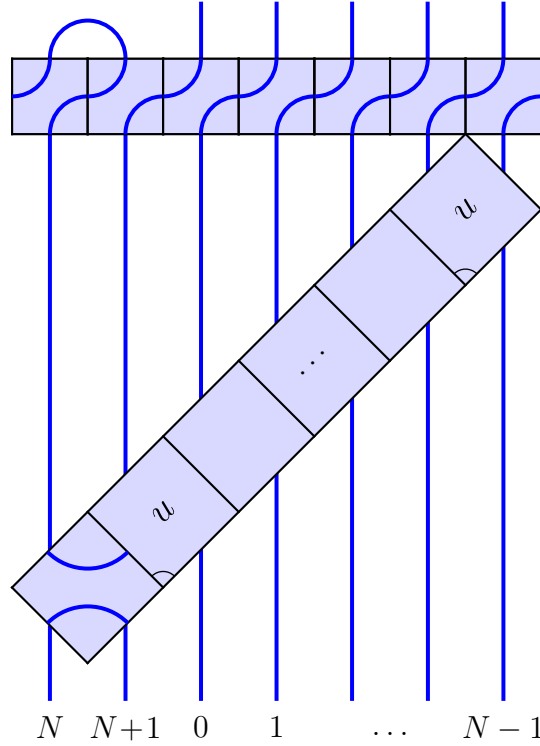


Figure 2: Diagrammatic representation of the single-row transfer matrix built from the enlarged periodic TL algebra acting on $N + 2$ strings.

for example, the six augmented DC link states are given by

$$\text{Diagrammatic link states} \quad (3.17)$$

where the nodes are labelled from $j = 0$ to $j = N + 1$. For $N = 3$, and an arbitrary odd number of defects, we have four augmented link states

$$\text{Diagrammatic link states} \quad (3.18)$$

where the nodes are labelled, as before, from $j = 0$ to $j = N + 1$.

To further facilitate the implementation of the analysis on a computer, we note that the link states can be described as sets of pairs of connecting arcs and defects. In this language, the set of link states (3.14) reads

$$\{\{1\}, \{2, 3\}\}, \{\{1, 2\}, \{3\}\}, \{\{2\}, \{3, 1\}\} \quad (3.19)$$

4 Inversion Identities

Remarkably, the transfer matrix (3.1) satisfies an inversion identity in the cylinder TL algebra. This identity is thus independent of the choice of vector space of link states eventually acted on to form a matrix representation. First, we describe the identity in the general cylinder setting (and prove it in Appendix A.1). We then characterize it when acting on the various link states introduced above. The inversion identity is unique to critical dense polymers among the logarithmic minimal models [6]. The analogous inversion identity for critical dense polymers on the *strip* is discussed in [8]. Although the inversion identities on the strip and the cylinder have common features, their solutions and general properties are very different.

4.1 Cylinder inversion identity

In preparation for the inversion identity, we introduce the two 3-tangles

$$- \begin{array}{|c|} \hline \text{---} \\ \hline \end{array} \quad \text{and} \quad \begin{array}{|c|} \hline \text{---} \\ \hline \end{array} \quad (4.1)$$

as they play important roles as building blocks in the following. The N -tangle \mathbf{J} , in particular, is defined as the sum of the 2^N possible horizontal combinations of N of these 3-tangles, where the left and right edges are identified to respect the cylinder topology. Due to the minus sign in (4.1), exactly half of the terms in \mathbf{J} appear with a minus sign. For small N , we thus have

$$\mathbf{J}|_{N=1} = - \begin{array}{|c|} \hline \text{---} \\ \hline \end{array} + \begin{array}{|c|} \hline \text{---} \\ \hline \end{array} = -\Omega^2 + \Omega^{-2} \quad (4.2)$$

$$\mathbf{J}|_{N=2} = \Omega^2 - \begin{array}{|c|} \hline \text{---} \\ \hline \end{array} - \begin{array}{|c|} \hline \text{---} \\ \hline \end{array} + \Omega^{-2} \quad (4.3)$$

$$\begin{aligned} \mathbf{J}|_{N=3} = & -\Omega^2 + \begin{array}{|c|} \hline \text{---} \\ \hline \end{array} + \begin{array}{|c|} \hline \text{---} \\ \hline \end{array} + \begin{array}{|c|} \hline \text{---} \\ \hline \end{array} \\ & - \begin{array}{|c|} \hline \text{---} \\ \hline \end{array} - \begin{array}{|c|} \hline \text{---} \\ \hline \end{array} - \begin{array}{|c|} \hline \text{---} \\ \hline \end{array} + \Omega^{-2} \end{aligned} \quad (4.4)$$

Although the N -tangle $\mathbf{J} = \mathbf{J}(\alpha)$ depends on the fugacity α of non-contractible loops, it is independent of the spectral parameter u .

Inversion Identity *The N -tangle $\mathbf{T}(u)$ defined in (3.1) satisfies*

$$\mathbf{T}(u)\mathbf{T}(u + \frac{\pi}{2}) = (\cos^{2N} u + (-1)^N \sin^{2N} u)\mathbf{I} + (\cos u \sin u)^N \mathbf{J} \quad (4.5)$$

The proof of this Inversion Identity is provided in Appendix A.1.

It follows from the inversion identity (4.5) and the commutativity property (3.3) that \mathbf{J} is a *symmetry* of the model in the sense that it commutes with the transfer matrix,

$$[\mathbf{J}, \mathbf{T}(u)] = [\mathbf{J}, \Omega^{\pm 1}] = 0 \quad (4.6)$$

As discussed in Section 4.3, \mathbf{J} is related to the so-called braid transfer matrices.

4.2 Matrix realization of \mathbf{J}

Obtaining a matrix realization of \mathbf{J} is greatly simplified by the Drop-Down Lemma below. To state it, we introduce the *arc-part* of a link state as the part remaining when ignoring all defects. For given number of nodes N , a (DC or IC) link state is thus characterized completely by its arc-part and its number of defects. The arc-part of any of the three link states in (3.14) consists of a single half-arc whose position depends on the original link state. We also say that the arc-part of a link state is *contained* in the arc-part of another link state if the bigger arc-part can be constructed from the smaller one by addition of half-arcs. Two identical arc-parts are said to be contained in each other.

Drop-Down Lemma *The action of \mathbf{J} on a given input link state results in link states whose arc-part contains the arc-part of the input link state.*

The proof of this Drop-Down Lemma is provided in Appendix A.2.

So far, we have not specified the class of link states which \mathbf{J} is acting on. The following Sector Lemma concerns the matrix realization of \mathbf{J} in a given sector.

Sector Lemma *In a given sector defined by a specified number of defects ℓ , the matrix realization of \mathbf{J} is diagonal and given by*

$$\mathbf{J} = \begin{cases} (-1)^{\frac{N-\ell}{2}} (2 + (\alpha^2 - 4)\delta_{\ell,0}) \mathbf{I}, & N, \ell \text{ even} \\ 0, & N, \ell \text{ odd} \end{cases} \quad (4.7)$$

The proof of this Sector Lemma is provided in Appendix A.3.

It is also of interest to examine the action of \mathbf{J} on the set of link states with an *arbitrary* number of defects. After completion of the drop-down process, the remaining part of the link state consists of defects only and the situation is equivalent to a scenario with system size $N_\ell = \ell$ where ℓ is the number of defects of the original input link state. That is, all the essential data is encoded in the Drop-Down Lemma and the action of \mathbf{J} on link states with defects only. It is noted that this is true for all sectors or combinations thereof, in particular for the union of all sectors of the parity of N .

As discussed in Appendix A.4, the matrix realization of \mathbf{J} acting on the set of link states with an *arbitrary odd number* of defects is the *zero matrix*. For N even, on the other hand, the matrix realization of \mathbf{J} acting on the set of link states with an *arbitrary even number* of defects is not diagonal, not even diagonalizable. With respect to the number of defects, the matrix is upper block triangular. The blocks on the diagonal are the same as the ones obtained by the sector-by-sector analysis above, while the entries outside these blocks give rise to a non-trivial Jordan decomposition. In particular, for DC link states with $\alpha = 2$ and $N = 8, 10, 12, 14$, we observe that Jordan blocks of rank 2 appear, but not of higher rank, while there are no rank-2 blocks for the smallest system sizes $N = 2, 4, 6$. Assuming that no Jordan blocks of rank 3 or higher occur for $N \geq 16$, we *conjecture* that the minimal polynomial identity satisfied by \mathbf{J} , valid for all even N , is

$$(\mathbf{J}^2 - 4\mathbf{I})^2 = 0, \quad \alpha = 2 \quad (4.8)$$

Such a minimal condition implies the existence of the (diagonalizable) *involution*

$$\mathbf{R} = -\frac{1}{16}(\mathbf{J}^3 - 12\mathbf{J}), \quad \mathbf{R}^2 = \mathbf{I} \quad (4.9)$$

The eigenvalues are $R = \frac{1}{2}J = \pm 1$. We will comment on this involution in Section 9, and refer to Appendix A.4 for additional details on the matrix realization of \mathbf{J} when acting on DC link states with an arbitrary number of defects.

4.3 Braid limits

Let us define the braid limits by

$$b^\pm = \lim_{u \rightarrow \pm i\infty} \frac{X(u)}{\sin(u + \frac{\pi}{4})} = e^{\mp \frac{\pi i}{4}} \begin{array}{|c|} \hline \text{[Diagram: Square with blue background and a blue arc from bottom-left to top-right]} \\ \hline \end{array} + e^{\pm \frac{\pi i}{4}} \begin{array}{|c|} \hline \text{[Diagram: Square with blue background and a blue arc from top-left to bottom-right]} \\ \hline \end{array}, \quad \mathbf{B}^\pm = \lim_{u \rightarrow \pm i\infty} \frac{\mathbf{T}(u)}{\sin^N(u + \frac{\pi}{4})} \quad (4.10)$$

By taking the braid limit of (4.5), the matrix \mathbf{J} is seen to be simply related to the braid transfer matrices \mathbf{B}^\pm

$$(\mathbf{B}^\pm)^2 = 2\mathbf{I} + (\pm i)^N \mathbf{J} \quad (4.11)$$

Using that $\mathbf{J} = 0$ for N odd, we find

$$(\mathbf{B}^\pm)^2 = \begin{cases} 2\mathbf{I} + (-1)^{\frac{N}{2}} \mathbf{J}, & N \text{ even} \\ 2\mathbf{I}, & N \text{ odd} \end{cases}, \quad \mathbf{J} = \begin{cases} (-1)^{\frac{N}{2}} ((\mathbf{B}^\pm)^2 - 2\mathbf{I}), & N \text{ even} \\ 0, & N \text{ odd} \end{cases} \quad (4.12)$$

Assuming the conjectured minimal polynomial identity (4.8) for \mathbf{J} implies that $\mathbf{B} = \mathbf{B}^\pm$ satisfies

$$\mathbf{B}^4(\mathbf{B}^2 - 4\mathbf{I})^2 = 0, \quad N \text{ even}; \quad \mathbf{B}^2 = 2\mathbf{I}, \quad N \text{ odd} \quad (4.13)$$

The eigenvalues of the braid matrices are thus of the form

$$B = 2 \cos \frac{s\pi}{4}, \quad s = 0, 1, 2, 3, 4 \quad (4.14)$$

where

$$B = 0, \pm 2, \quad N \text{ even}; \quad B = \pm\sqrt{2}, \quad N \text{ odd} \quad (4.15)$$

4.4 Matrix inversion identities

Once a matrix representation of $\mathbf{T}(u)$ has been fixed, the inversion identity (4.5) translates into a *matrix inversion identity*. Here, we consider the link states counted in (3.13), including the DC link states for $\ell = 0$ but not the IC link states. The latter are discussed in Section 4.5.

It follows from the Inversion Identity (4.5) and the Sector Lemma (4.7) that the matrix inversion identity for a given sector reads

$$\mathbf{T}(u)\mathbf{T}(u + \frac{\pi}{2}) = \left(\cos^{2N}u + \sin^{2N}u + (-1)^{\frac{N-\ell}{2}}(2 + (\alpha^2 - 4)\delta_{\ell,0})(\cos u \sin u)^N \right) \mathbf{I} \quad (4.16)$$

for N even, while for N odd, it reads

$$\mathbf{T}(u)\mathbf{T}(u + \frac{\pi}{2}) = (\cos^{2N}u - \sin^{2N}u) \mathbf{I} \quad (4.17)$$

In order to solve the inversion identity (4.16) for the associated eigenvalues (N even), we choose to focus on particular values for α in the following. For $\alpha^2 = 4$, we thus have the matrix inversion identities

$$\mathbf{T}(u)\mathbf{T}(u + \frac{\pi}{2}) = (\cos^N u + (-1)^{\frac{N-\ell}{2}} \sin^N u)^2 \mathbf{I} \quad (4.18)$$

while, for $\alpha = 0$ and $\ell = 0$, we have

$$\mathbf{T}(u)\mathbf{T}(u + \frac{\pi}{2}) = (\cos^N u - (-1)^{\frac{N}{2}} \sin^N u)^2 \mathbf{I} \quad (4.19)$$

We find that

$$\alpha = 2 \quad (4.20)$$

is the most natural value for the fugacity of non-contractible loops.

4.5 Identified connectivities

The distinction between DC and IC link states is only meaningful for link states without defects. In this case, the number of IC link states is smaller than the number of DC link states, cf. (3.12), implying that, for given N , the corresponding matrix realization of $\mathbf{T}(u)$ or \mathbf{J} is of lower dimension in the IC case than in the DC case. As already mentioned, the appropriate algebra in the IC case is the enlarged TL algebra with $\alpha = \beta = 0$. It follows that the matrix inversion identity takes the same form as (4.19), namely

$$\mathbf{T}(u)\mathbf{T}(u + \frac{\pi}{2}) = (\cos^N u - (-1)^{\frac{N}{2}} \sin^N u)^2 \mathbf{I} \quad (4.21)$$

but applies to matrices of smaller dimension than the ones appearing in (4.19).

5 Solution on a Finite Cylinder

In this section, we solve the inversion identities for the transfer matrix eigenvalues on finite-size cylinders sector by sector for $\alpha = 2$. We also discuss the relation, through finite-size corrections, to the conformal partition functions. The methods build on the previous works [13], [21] and [8].

The key idea is that the eigenvalues $T(u)$ of the transfer matrices in a given sector are determined, up to an overall constant ρ , by the positions u_j of their zeros in the analyticity strip $-\pi/4 \leq \text{Re } u < 3\pi/4$

$$T(u) = \rho \prod_{j=1}^N \sin(u - u_j) \quad (5.1)$$

These eigenvalues are Laurent polynomials in $z = e^{iu}$. Given a (right) eigenvector independent of u , this follows since each entry of the transfer matrix is of this form. This argument, which applies to the action of the transfer matrix on a particular eigenvector, holds even if the commuting transfer matrices are not diagonalizable. Typically, in the ℓ even sectors on the cylinder, we find that the transfer matrices are not diagonalizable as we find Jordan blocks of rank 2. We have not found Jordan blocks of any higher rank. Moreover, we find, in a given ℓ sector, that all of the eigenvectors (excluding generalized eigenvectors) are independent of u . Degenerate eigenvalues are exactly degenerate as Laurent polynomials so such eigenvalues occur with degeneracy 2. These observations enable us to numerically obtain all of the eigenvalues as Laurent polynomials in $z = e^{iu}$.

We emphasize that this situation on the cylinder is in contrast to critical dense polymers on the strip in sectors of the extended Kac table for which the transfer matrices are found empirically [8] to be simultaneously diagonalizable. It seems that it is not possible to avoid reducible yet indecomposable representations of rank 2 in the ℓ even sectors on the cylinder.

5.1 Finite-size corrections

The partition function of critical dense polymers on a periodic lattice of N columns and M rows is defined by

$$Z_{N,M} = \text{Tr } \mathbf{T}(u)^M = \sum_{n \geq 0} T_n(u)^M = \sum_{n \geq 0} e^{-M \mathcal{E}_n(u)} \quad (5.2)$$

Here the sum is over all eigenvalues of $\mathbf{T}(u)$, including possible multiplicities, and $\mathcal{E}_n(u)$ with $n = 0, 1, 2, \dots$ is the energy associated to the eigenvalue $T_n(u)$. The maximal eigenvalue $T_0(u)$ is labelled by $n = 0$. The maximal eigenvalue in the sector with ℓ defects is denoted by $T_{0,\ell}(u)$. Conformal invariance of the model in the continuum scaling limit dictates [22, 23] that the leading finite-size corrections for large N are of the form

$$\begin{aligned} \mathcal{E}_0 &= N f_{bulk} - \frac{\pi c}{6N} \sin \vartheta \\ \mathcal{E}_n - \mathcal{E}_0 &= \frac{2\pi i}{N} [(\Delta + k)e^{-i\vartheta} - (\bar{\Delta} + \bar{k})e^{i\vartheta}] \\ &= \frac{2\pi}{N} [(\Delta + \bar{\Delta} + k + \bar{k}) \sin \vartheta + i(\Delta - \bar{\Delta} + k - \bar{k}) \cos \vartheta] \end{aligned} \quad (5.3)$$

Here f_{bulk} is the bulk free energy per face [8]

$$f_{bulk} = \frac{1}{2} \log 2 - \frac{1}{\pi} \int_0^{\pi/2} \log \left(\frac{1}{\sin t} + \sin 2u \right) dt \quad (5.4)$$

and $\vartheta = 2u$ is the anisotropy angle. The conformal spectrum is determined by the central charge $c = -2$, the conformal weights $\Delta, \bar{\Delta}$ and the excitations or descendants labelled by the non-negative integers k, \bar{k} . The conformal weights are given by

$$\Delta = \Delta_t = \frac{t^2 - 1}{8}, \quad t \in \frac{1}{2}\mathbb{Z} \quad (5.5)$$

where t can be integer or half-integer

$$\Delta = \begin{cases} \Delta_{r,s} = \Delta_{2r-s} \in \{-\frac{1}{8}, 0, \frac{3}{8}, 1, \frac{15}{8}, \dots\}, & r \in \mathbb{N}, s = 1, 2; & N \text{ even} \\ \Delta_t \in \{-\frac{3}{32}, \frac{5}{32}, \frac{21}{32}, \frac{45}{32}, \frac{77}{32}, \frac{117}{32}, \dots\}, & t \in \mathbb{Z} - \frac{1}{2}; & N \text{ odd} \end{cases} \quad (5.6)$$

Here r, s are the Kac labels [8] and $t = \ell/2$ where ℓ is the number of defects. The Kac table is shown in Figure 3.

In the scaling limit, the conformal partition functions are sesquilinear forms in characters

$$Z(q) = \sum_{\Delta, \bar{\Delta}} \mathcal{N}_{\Delta, \bar{\Delta}} \chi_{\Delta}(q) \chi_{\bar{\Delta}}(\bar{q}) \quad (5.7)$$

where the characters are of the form

$$\chi_{\Delta}(q) = q^{-c/24} \sum_{k=0}^{\infty} d_{\Delta}(k) q^{\Delta+k} = \begin{cases} \text{ch}_{r,s}(q) = \frac{q^{-c/24+\Delta_{r,s}}(1-q^{rs})}{\prod_{n=1}^{\infty} (1-q^n)}, & N \text{ even} \\ \text{ch}_t(q) = \frac{q^{-c/24+\Delta_t}}{\prod_{n=1}^{\infty} (1-q^n)}, & N \text{ odd} \end{cases} \quad (5.8)$$

s	\vdots	\vdots	\vdots	\vdots	\vdots	\vdots	\dots
10	$\frac{63}{8}$	$\frac{35}{8}$	$\frac{15}{8}$	$\frac{3}{8}$	$-\frac{1}{8}$	$\frac{3}{8}$	\dots
9	6	3	1	0	0	1	\dots
8	$\frac{35}{8}$	$\frac{15}{8}$	$\frac{3}{8}$	$-\frac{1}{8}$	$\frac{3}{8}$	$\frac{15}{8}$	\dots
7	3	1	0	0	1	3	\dots
6	$\frac{15}{8}$	$\frac{3}{8}$	$-\frac{1}{8}$	$\frac{3}{8}$	$\frac{15}{8}$	$\frac{35}{8}$	\dots
5	1	0	0	1	3	6	\dots
4	$\frac{3}{8}$	$-\frac{1}{8}$	$\frac{3}{8}$	$\frac{15}{8}$	$\frac{35}{8}$	$\frac{63}{8}$	\dots
3	0	0	1	3	6	10	\dots
2	$-\frac{1}{8}$	$\frac{3}{8}$	$\frac{15}{8}$	$\frac{35}{8}$	$\frac{63}{8}$	$\frac{99}{8}$	\dots
1	0	1	3	6	10	15	\dots
	1	2	3	4	5	6	r

Figure 3: Kac table of the ℓ even sectors of critical dense polymers. The relevant rows, $s = 1$ and $s = 2$, label the Neveu-Schwarz and Ramond sectors, respectively. The (r, s) representations indicated with a red quadrant are irreducible representations with characters $\chi_{r,s}(q) = \text{ch}_{r,s}(q)$.

and $d_{\Delta}(k)$ are the degeneracies at level k . The modular nome is

$$q = \exp(2\pi i\tau), \quad \tau = \frac{M}{N} \exp[i(\pi - \vartheta)] = -\delta e^{-2iu} \quad (5.9)$$

$$\bar{q} = \exp(-2\pi i\bar{\tau}), \quad \bar{\tau} = \frac{M}{N} \exp[-i(\pi - \vartheta)] = -\delta e^{2iu} \quad (5.10)$$

$$|q|^2 = q\bar{q} = \exp(-4\pi\delta \sin 2u) \quad (5.11)$$

where $\delta = M/N$ is the aspect ratio and $\text{Im } \tau > 0$ in the physical strip $0 < \text{Re } u < \frac{\pi}{2}$. The characters $\text{ch}_{r,s}(q)$ with $s = 1, 2$ in the N even sectors are the characters of irreducible Kac representations [6] whereas $\text{ch}_t(q)$ in the N odd sectors are the characters of generic (irreducible) Virasoro modules.

5.2 \mathbb{Z}_4 sectors (N odd, ℓ odd)

In the \mathbb{Z}_4 sectors, the sector-by-sector inversion identity for the eigenvalues is

$$T(u)T(u + \frac{\pi}{2}) = \cos^{2N}u - \sin^{2N}u \quad (5.12)$$

Factorizing the right side gives

$$\cos^{2N}u - \sin^{2N}u = \frac{e^{-2Niu}}{2^{2N-1}} \prod_{j=1}^N \left(e^{4iu} + \tan^2 \frac{(2j-1)\pi}{4N} \right) \quad (5.13)$$

Sharing out the zeros to solve the functional equation, gives

$$T(u) = \epsilon \frac{(-i)^{N/2} e^{-Niu}}{2^{N-1/2}} \prod_{j=1}^N \left(e^{2iu} + i\epsilon_j \tan \frac{(2j-1)\pi}{4N} \right) \quad (5.14)$$

where $\epsilon^2 = \epsilon_j^2 = 1$. The ordinates of the locations of zeros are

$$y_j = -\frac{1}{2} \log \tan \frac{\frac{1}{2}(j - \frac{1}{2})\pi}{N}, \quad j = 1, 2, \dots, N \quad (5.15)$$

A typical pattern of zeros is shown in Figure 4.

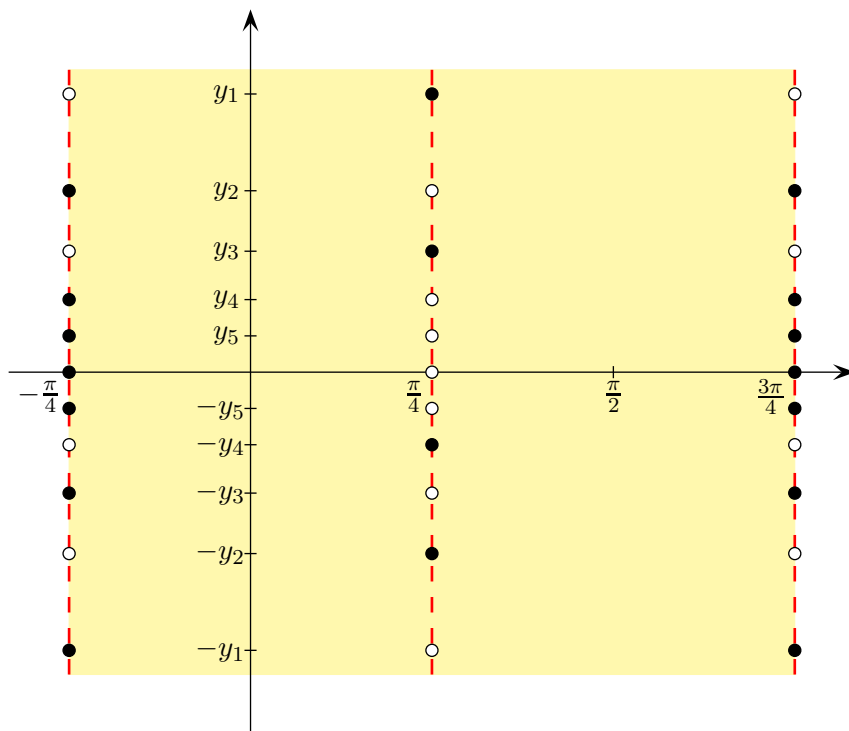


Figure 4: A typical pattern of zeros in the complex u -plane for the \mathbb{Z}_4 sectors (N odd, ℓ odd). Here, $N = 11$ and $\ell = 7$. The ordinates of the locations of the zeros u_j are $y_j = -\frac{1}{2} \log \tan \frac{(2j-1)\pi}{4N}, j = 1, 2, \dots, N$. At each position j , there is either a 1-string with $\text{Re } u_j = \pi/4$ or a 2-string with $\text{Re } u_j = -\pi/4, 3\pi/4$.

We see that these solutions (eigenvalues) satisfy the crossing symmetry

$$\overline{T\left(\frac{\pi}{2} - \bar{u}\right)} = T(u) \quad (5.16)$$

The choice $\epsilon_j = -1$ for a particular j corresponds to an elementary excitation. In principle, up to the overall choice of sign ϵ , there are 2^N possible eigenvalues allowing for all excitations. However, only $\binom{N}{\frac{N-\ell}{2}}$ of these solutions actually occur as eigenvalues and these are determined by selection rules as explained in Section 7. For $\ell = 1$, the largest eigenvalue $T_{0,1}(u)$ occurs for $\epsilon_j = 1$ for all $j = 1, 2, \dots, N$, that is, there are 2-strings at each position j and no 1-strings. The patterns of zeros of $T(u)$ are conveniently encoded by introducing pairs of

single-column diagrams as shown in Figure 5. The right column corresponds to the 1-strings in the lower-half u -plane (associated with \bar{q}). The left column corresponds to the 1-strings in the upper half-plane (associated with q), including the real axis, but rotated through 180 degrees. Positions occupied by a 1-string are indicated by a solid circle and unoccupied positions are indicated by an open circle. For N odd and ℓ odd, the patterns of zeros of $T_{0,\ell}(u)$ are shown in Figure 6.

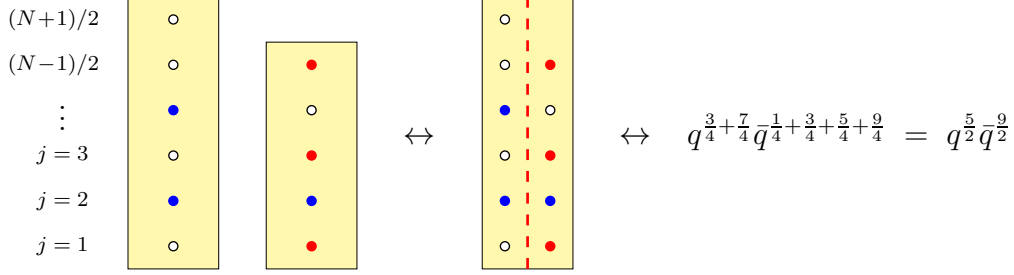


Figure 5: The patterns of zeros of $T(u)$ in the \mathbb{Z}_4 sectors are encoded by introducing pairs of single-column diagrams. The right column corresponds to the 1-strings in the lower-half u -plane (associated with \bar{q}). The left column corresponds to the 1-strings in the upper half-plane (associated with q), including the real axis, but rotated through 180 degrees. Positions occupied by a 1-string are indicated by a solid circle and unoccupied positions are indicated by an open circle. The 1-string energies are given by $E_j = \frac{1}{2}(j - \frac{1}{2})$. Here, $N = 11$, $\sigma = 2$, $\bar{\sigma} = -2$ and $\ell = 2(\sigma + \bar{\sigma}) + 1 = 1$.

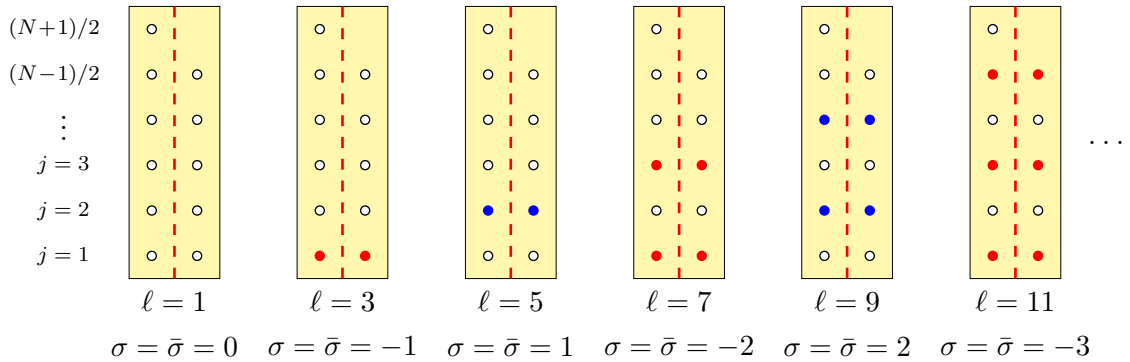


Figure 6: Groundstate configurations in the \mathbb{Z}_4 sectors with ℓ defects (N, ℓ odd). The quantum numbers $\sigma, \bar{\sigma}$ are as shown and the conformal weights are $(\Delta, \bar{\Delta}) = (\Delta_{\ell/2}, \Delta_{\ell/2})$.

Next, we separate the contribution from zeros in the upper and lower half-planes by keeping ϵ_j for $j = 1, 2, \dots, (N + 1)/2$ and setting

$$\bar{\epsilon}_j = \epsilon_{N+1-j} = \pm 1, \quad j = 1, 2, \dots, \frac{N-1}{2} \quad (5.17)$$

By convention, we treat the zeros on the real axis labelled by $j = (N + 1)/2$ as if they are in the upper half-plane. Setting $\epsilon = \mu \prod_{j=1}^{(N-1)/2} \bar{\epsilon}_j$ gives

$$T(u) = \frac{\mu (-i)^{N/2}}{2^{N-1/2} e^{Niu}} \prod_{j=1}^{\frac{N+1}{2}} \left(e^{2iu} + i\epsilon_j \tan \frac{(2j-1)\pi}{4N} \right) \prod_{j=1}^{\frac{N-1}{2}} \left(\bar{\epsilon}_j e^{2iu} + i \cot \frac{(2j-1)\pi}{4N} \right) \quad (5.18)$$

We fix $\mu = +1$ to ensure that $T_{0,1}(0) = 1$ consistent with (3.2). Taking the ratio of (5.18) with precisely one $\epsilon_j = -1$ or $\bar{\epsilon}_j = -1$ to (5.18) with all $\epsilon_j = \bar{\epsilon}_j = +1$, and then taking the limit with a fixed aspect ratio $\delta = M/N$, gives

$$\lim_{M,N \rightarrow \infty} \left(\frac{e^{2iu} - i \tan \frac{(2j-1)\pi}{4N}}{e^{2iu} + i \tan \frac{(2j-1)\pi}{4N}} \right)^M = \exp[-(j - \frac{1}{2})\pi i \delta e^{-2iu}] = q^{E_j} \quad (5.19)$$

$$\lim_{M,N \rightarrow \infty} \left(\frac{-e^{2iu} + i \cot \frac{(2j-1)\pi}{4N}}{e^{2iu} + i \cot \frac{(2j-1)\pi}{4N}} \right)^M = \exp[(j - \frac{1}{2})\pi i \delta e^{2iu}] = \bar{q}^{E_j} \quad (5.20)$$

where

$$E_j = \frac{1}{2}(j - \frac{1}{2}), \quad N, \ell \text{ odd} \quad (5.21)$$

It follows that the conformal partition function in the \mathbb{Z}_4 sectors with ℓ defects is

$$Z_\ell(q) = (q\bar{q})^{-c/24 + \Delta_{1/2}} \sum_{\epsilon, \bar{\epsilon}} q^{\sum_{j=1}^{(N+1)/2} \delta(\epsilon_j, -1) E_j} \bar{q}^{\sum_{j=1}^{(N-1)/2} \delta(\bar{\epsilon}_j, -1) E_j} \quad (5.22)$$

where the sum and the allowed values of ϵ_j and $\bar{\epsilon}_j$ are determined by selection rules as explained in Section 7. Here $\delta(j, k) = \delta_{j,k}$ is the Kronecker delta. The prefactor involving the central charge and conformal weights comes from the largest eigenvalue $T_{0,\ell}(u)$ with $\ell = 1$ and is obtained by applying Euler-Maclaurin as explained in Section 6.

5.3 Ramond and Neveu-Schwarz sectors (N even, ℓ even)

In the ℓ even sectors, the sector-by-sector inversion identity for the eigenvalues is

$$T(u)T(u + \frac{\pi}{2}) = (\cos^N u + (-1)^{(N-\ell)/2} \sin^N u)^2 \quad (5.23)$$

Using the identities

$$\cos^N u + (-1)^{N/2} \sin^N u = \frac{e^{-Niu}}{2^{N-1}} \prod_{j=1}^{N/2} \left(e^{4iu} + \tan^2 \frac{(2j-1)\pi}{2N} \right), \quad \ell/2 \text{ even} \quad (5.24)$$

$$\cos^N u - (-1)^{N/2} \sin^N u = \frac{N e^{(2-N)iu}}{2^{N-1}} \prod_{j=1}^{N/2-1} \left(e^{4iu} + \tan^2 \frac{j\pi}{N} \right), \quad \ell/2 \text{ odd} \quad (5.25)$$

we see that for the two parities of $\ell/2$

$$\begin{aligned} (\cos^N u + (-1)^{N/2} \sin^N u)^2 &= \frac{e^{-2Niu}}{2^{2N-2}} \prod_{j=1}^{N/2} \left(e^{2iu} + i\epsilon_j \tan \frac{(2j-1)\pi}{2N} \right) \left(e^{2iu} - i\epsilon_j \tan \frac{(2j-1)\pi}{2N} \right) \\ &\times \prod_{j=1}^{N/2} \left(e^{2iu} + i\mu_j \tan \frac{(2j-1)\pi}{2N} \right) \left(e^{2iu} - i\mu_j \tan \frac{(2j-1)\pi}{2N} \right) \end{aligned} \quad (5.26)$$

$$\begin{aligned} (\cos^N u - (-1)^{N/2} \sin^N u)^2 &= \frac{N^2 e^{(4-2N)iu}}{2^{2N-2}} \prod_{j=1}^{N/2-1} \left(e^{2iu} + i\epsilon_j \tan \frac{j\pi}{N} \right) \left(e^{2iu} - i\epsilon_j \tan \frac{j\pi}{N} \right) \\ &\times \prod_{j=1}^{N/2-1} \left(e^{2iu} + i\mu_j \tan \frac{j\pi}{N} \right) \left(e^{2iu} - i\mu_j \tan \frac{j\pi}{N} \right) \end{aligned} \quad (5.27)$$

where $\epsilon_j^2 = \mu_j^2 = 1$. Sharing out the zeros to solve the functional equation, gives

$$T(u) = \begin{cases} \frac{\epsilon(-i)^{\frac{N}{2}} e^{-Niu}}{2^{N-1}} \prod_{j=1}^{N/2} \left(e^{2iu} + i\epsilon_j \tan \frac{(2j-1)\pi}{2N} \right) \left(e^{2iu} + i\mu_j \tan \frac{(2j-1)\pi}{2N} \right), & \frac{\ell}{2} \text{ even} \\ \frac{\epsilon(-i)^{\frac{N-2}{2}} N e^{(2-N)iu}}{2^{N-1}} \prod_{j=1}^{N/2-1} \left(e^{2iu} + i\epsilon_j \tan \frac{j\pi}{N} \right) \left(e^{2iu} + i\mu_j \tan \frac{j\pi}{N} \right), & \frac{\ell}{2} \text{ odd} \end{cases} \quad (5.28)$$

We see that these solutions (eigenvalues) satisfy the crossing symmetry

$$\overline{T\left(\frac{\pi}{2} - \bar{u}\right)} = T(u) \quad (5.29)$$

The ordinates of the locations of zeros are

$$y_j = \begin{cases} -\frac{1}{2} \log \tan \frac{(j-\frac{1}{2})\pi}{N}, & \ell/2 \text{ even}, j = 1, 2, \dots, N/2 \\ -\frac{1}{2} \log \tan \frac{j\pi}{N}, & \ell/2 \text{ odd}, j = 1, 2, \dots, N/2 - 1 \end{cases} \quad (5.30)$$

A typical pattern of zeros is shown in Figure 7.

The choice $\epsilon_j = -1$ or $\mu_j = -1$ for a particular j corresponds to an elementary excitation. In principle, up to the overall choice of sign ϵ , there are either 2^N or 2^{N-2} possible eigenvalues allowing for all excitations. However, only $\binom{N-\ell}{2}$ of these solutions actually occur as eigenvalues and these are determined by selection rules as explained in Section 7. For $\ell = 0$, the largest eigenvalue $T_{0,0}(u)$ occurs for $\epsilon_j = \mu_j = 1$ for all $j = 1, 2, \dots, N$, that is, there are 2-strings at each position j and no 1-strings. The patterns of zeros of $T(u)$ are conveniently encoded by introducing pairs of double-column diagrams as shown in Figures 8 and 10. The right column corresponds to the 1-strings in the lower-half u -plane (associated with \bar{q}). The left column corresponds to the 1-strings in the upper half-plane (associated with q), including the real axis, but rotated through 180 degrees. Positions occupied by a 1-string are indicated by a solid circle and unoccupied positions are indicated by an open circle. For N even and $\ell/2$ even or odd, the patterns of zeros of $T_{0,\ell}(u)$ are shown in Figures 9 and 11.

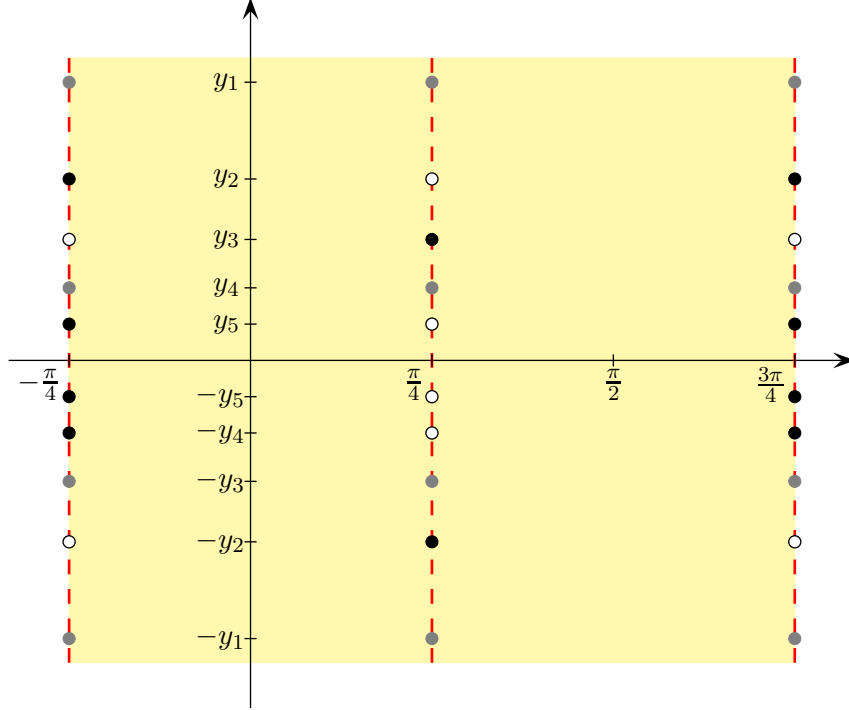


Figure 7: A typical pattern of zeros in the complex u -plane for the ℓ even sectors. Here, $N = 12$ and $\ell = 2$. The ordinates of the locations of the zeros u_j are $y_j = -\frac{1}{2} \log \tan \frac{j\pi}{N}$, $j = 1, 2, \dots, N/2 - 1$. At each position j , there is either two 1-strings with $\text{Re } u_j = \pi/4$, two 2-strings with real parts $\text{Re } u_j = -\pi/4, 3\pi/4$ or one 1-string and one 2-string. A double zero is indicated by a black circle, a single zero by a grey circle and an unoccupied position by an open circle.

Next, we separate the contribution from zeros in the upper and lower half-planes. For $\ell/2$ even, we keep ϵ_j and μ_j for $j = 1, 2, \dots, \lfloor (N+2)/4 \rfloor$ and set

$$\bar{\epsilon}_j = \epsilon_{N/2+1-j} = \pm 1, \quad j = 1, 2, \dots, \lfloor N/4 \rfloor \quad (5.31)$$

$$\bar{\mu}_j = \mu_{N/2+1-j} = \pm 1, \quad j = 1, 2, \dots, \lfloor N/4 \rfloor \quad (5.32)$$

For $\ell/2$ odd, we keep ϵ_j and μ_j for $j = 1, 2, \dots, \lfloor N/4 \rfloor$ and set

$$\bar{\epsilon}_j = \epsilon_{N/2-j} = \pm 1, \quad j = 1, 2, \dots, \lfloor (N-2)/4 \rfloor \quad (5.33)$$

$$\bar{\mu}_j = \mu_{N/2-j} = \pm 1, \quad j = 1, 2, \dots, \lfloor (N-2)/4 \rfloor \quad (5.34)$$

By convention, we treat the zeros on the real axis (labelled by $j = (N+2)/4$ in the case $\ell/2$ even and $N = 2 \pmod{4}$ and by $j = N/4$ in the case $\ell/2$ odd and $N = 0 \pmod{4}$) as if they are in the upper half-plane. For $\ell/2$ even, setting $\epsilon = \mu \prod_{j=1}^{\lfloor N/4 \rfloor} \bar{\epsilon}_j \bar{\mu}_j$ gives

$$\begin{aligned} T(u) &= \frac{\mu(-i)^{\frac{N}{2}} e^{-Niu}}{2^{N-1}} \prod_{j=1}^{\lfloor (N+2)/4 \rfloor} \left(e^{2iu} + i\epsilon_j \tan \frac{(2j-1)\pi}{2N} \right) \left(\bar{\epsilon}_j e^{2iu} + i \cot \frac{(2j-1)\pi}{2N} \right) \\ &\times \prod_{j=1}^{\lfloor N/4 \rfloor} \left(e^{2iu} + i\mu_j \tan \frac{(2j-1)\pi}{2N} \right) \left(\bar{\mu}_j e^{2iu} + i \cot \frac{(2j-1)\pi}{2N} \right) \end{aligned} \quad (5.35)$$

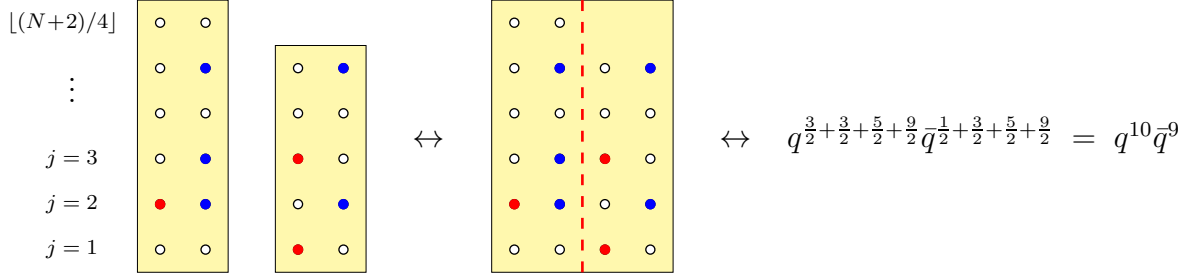


Figure 8: The patterns of zeros of $T(u)$ in the Ramond sectors (N even, $\ell/2$ even) are encoded by introducing pairs of double-column diagrams. The right double-column corresponds to the 1-strings in the lower-half u -plane (associated with \bar{q}). The left double-column corresponds to the 1-strings in the upper half-plane (associated with q), including the real axis, but rotated through 180 degrees. At each position in a double-column diagram, there are 0, 1 or 2 1-strings. Positions occupied by a 1-string are indicated by a solid circle and unoccupied positions are indicated by an open circle. The 1-string energies are given by $E_j = (j - \frac{1}{2})$. There are $\lfloor \frac{N+2}{4} \rfloor$ positions on the left and $\lfloor \frac{N}{4} \rfloor$ on the right. Here, $N = 22$, $\sigma = 2$, $\bar{\sigma} = 0$ and $\ell = 2(\sigma + \bar{\sigma}) = 4$.

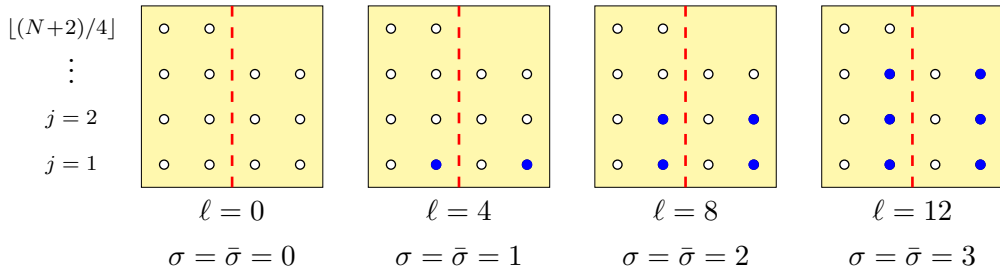


Figure 9: Groundstate configurations in the Ramond sectors with ℓ defects (N , $\ell/2$ even). Here $N = 14$, the quantum numbers $\sigma, \bar{\sigma}$ are as shown and the conformal weights are $(\Delta, \bar{\Delta}) = (\Delta_{\ell/2}, \Delta_{\ell/2})$.

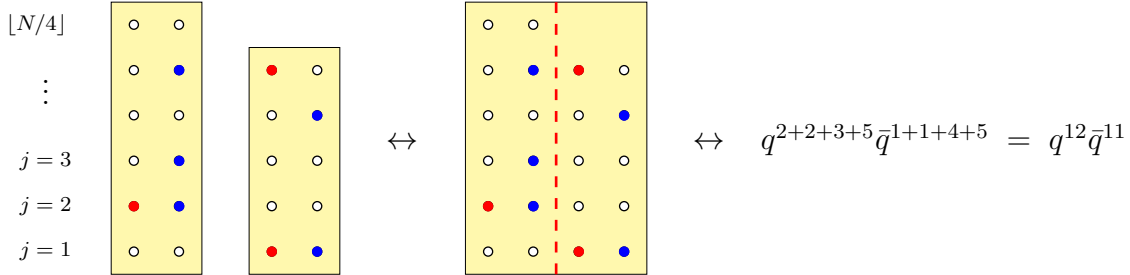


Figure 10: The patterns of zeros of $T(u)$ in the Neveu-Schwarz sectors (N even, $\ell/2$ odd) are encoded by introducing pairs of double-column diagrams. The right double-column corresponds to the 1-strings in the lower-half u -plane (associated with \bar{q}). The left double-column corresponds to the 1-strings in the upper half-plane (associated with q), including the real axis, but rotated through 180 degrees. At each position in a double-column diagram, there are 0, 1 or 2 1-strings. Positions occupied by a 1-string are indicated by a solid circle and unoccupied positions are indicated by an open circle. The 1-string energies are given by $E_j = j$. There are $\lfloor \frac{N}{4} \rfloor$ positions on the left and $\lfloor \frac{N-2}{4} \rfloor$ on the right. Here, $N = 24$, $\sigma = 2$, $\bar{\sigma} = 0$ and $\ell = 2(\sigma + \bar{\sigma} + 1) = 6$.

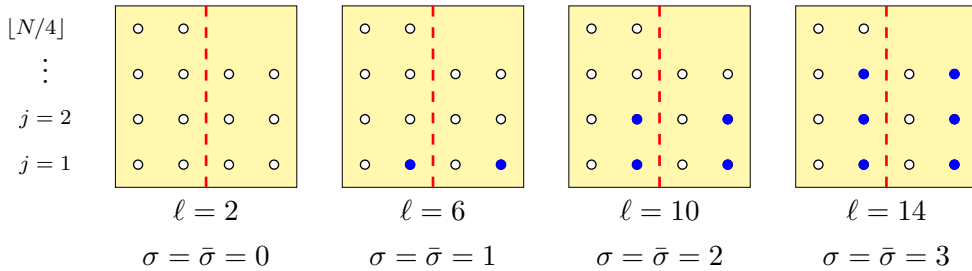


Figure 11: Groundstate configurations in the Neveu-Schwarz sectors with ℓ defects (N even, $\ell/2$ odd). Here $N = 16$, the quantum numbers $\sigma, \bar{\sigma}$ are as shown and the conformal weights are $(\Delta, \bar{\Delta}) = (\Delta_{\ell/2}, \Delta_{\ell/2})$.

For $\ell/2$ odd, setting $\epsilon = \mu \prod_{j=1}^{\lfloor (N-2)/4 \rfloor} \bar{\epsilon}_j \bar{\mu}_j$ gives

$$\begin{aligned}
T(u) &= \frac{\mu(-i)^{\frac{N-2}{2}} N e^{(2-N)iu}}{2^{N-1}} \prod_{j=1}^{\lfloor N/4 \rfloor} \left(e^{2iu} + i\epsilon_j \tan \frac{j\pi}{N} \right) \left(\bar{\epsilon}_j e^{2iu} + i \cot \frac{j\pi}{N} \right) \\
&\times \prod_{j=1}^{\lfloor (N-2)/4 \rfloor} \left(e^{2iu} + i\mu_j \tan \frac{j\pi}{N} \right) \left(\bar{\mu}_j e^{2iu} + i \cot \frac{j\pi}{N} \right)
\end{aligned} \tag{5.36}$$

Fixing $\mu = +1$ ensures that $T_{0,0}(0) = T_{0,2}(0) = 1$ consistent with (3.2). For $\ell/2$ even, taking the ratio of (5.35) with precisely one $\epsilon_j, \bar{\epsilon}_j$ or $\mu_j, \bar{\mu}_j = -1$ to (5.35) with all $\epsilon_j = \mu_j = \bar{\epsilon}_j = \bar{\mu}_j = +1$ and taking the limit $M, N \rightarrow \infty$ with a fixed aspect ratio $\delta = M/N$ gives

$$\lim_{M, N \rightarrow \infty} \left(\frac{e^{2iu} - i \tan \frac{(2j-1)\pi}{2N}}{e^{2iu} + i \tan \frac{(2j-1)\pi}{2N}} \right)^M = \exp[-(2j-1)\pi i \delta e^{-2iu}] = q^{E_j} \tag{5.37}$$

$$\lim_{M, N \rightarrow \infty} \left(\frac{-e^{2iu} + i \cot \frac{(2j-1)\pi}{2N}}{e^{2iu} + i \cot \frac{(2j-1)\pi}{2N}} \right)^M = \exp[(2j-1)\pi i \delta e^{2iu}] = \bar{q}^{E_j} \tag{5.38}$$

where $E_j = (j - \frac{1}{2})$. Similarly, for $\ell/2$ odd, taking the ratio of (5.36) with precisely one ϵ_j or $\mu_j = -1$ to (5.36) with all $\epsilon_j = \mu_j = \bar{\epsilon}_j = \bar{\mu}_j = +1$ and taking the limit $M, N \rightarrow \infty$ with a fixed aspect ratio $\delta = M/N$ gives

$$\lim_{M, N \rightarrow \infty} \left(\frac{e^{2iu} - i \tan \frac{j\pi}{N}}{e^{2iu} + i \tan \frac{j\pi}{N}} \right)^M = \exp[-2j\pi i \delta e^{-2iu}] = q^{E_j} \tag{5.39}$$

$$\lim_{M, N \rightarrow \infty} \left(\frac{-e^{2iu} + i \cot \frac{j\pi}{N}}{e^{2iu} + i \cot \frac{j\pi}{N}} \right)^M = \exp[2j\pi i \delta e^{2iu}] = \bar{q}^{E_j} \tag{5.40}$$

where $E_j = j$.

We conclude that, in the ℓ even sectors,

$$E_j = \begin{cases} j - \frac{1}{2}, & N \text{ even, } \ell/2 \text{ even} \\ j, & N \text{ even, } \ell/2 \text{ odd} \end{cases} \tag{5.41}$$

and the conformal partition functions are

$$Z_\ell(q) = \begin{cases} (q\bar{q})^{-c/24 + \Delta_0} \sum_{\epsilon, \mu, \bar{\epsilon}, \bar{\mu}} q^{\sum_{j=1}^{\lfloor \frac{N+2}{4} \rfloor} [\delta(\epsilon_j, -1) + \delta(\mu_j, -1)] E_j} \bar{q}^{\sum_{j=1}^{\lfloor \frac{N}{4} \rfloor} [\delta(\bar{\epsilon}_j, -1) + \delta(\bar{\mu}_j, -1)] E_j}, & \frac{\ell}{2} \text{ even} \\ (q\bar{q})^{-c/24 + \Delta_1} \sum_{\epsilon, \mu, \bar{\epsilon}, \bar{\mu}} q^{\sum_{j=1}^{\lfloor \frac{N}{4} \rfloor} [\delta(\epsilon_j, -1) + \delta(\mu_j, -1)] E_j} \bar{q}^{\sum_{j=1}^{\lfloor \frac{N-2}{4} \rfloor} [\delta(\bar{\epsilon}_j, -1) + \delta(\bar{\mu}_j, -1)] E_j}, & \frac{\ell}{2} \text{ odd} \end{cases} \tag{5.42}$$

where the sums and the allowed values of $\epsilon_j, \mu_j, \bar{\epsilon}_j, \bar{\mu}_j$ are determined by selection rules as explained in Section 7. The prefactor involving the central charge and conformal weights comes from the largest eigenvalue $T_{0,\ell}(u)$ with $\ell = 0, 2$ and is obtained by applying Euler-Maclaurin as explained in Section 6.

6 Finite-Size Corrections from Euler-Maclaurin

In this section, we use the Euler-Maclaurin formula to obtain the finite-size corrections for the following three groundstates

$$\begin{aligned}
T_{0,0}(u): \text{ Ramond } (N \text{ even}, \ell = 0) & \quad y_j = -\frac{1}{2} \log \tan \frac{(j - \frac{1}{2})\pi}{N} & \text{double} \\
T_{0,2}(u): \text{ Neveu-Schwarz } (N \text{ even}, \ell = 2) & \quad y_j = -\frac{1}{2} \log \tan \frac{j\pi}{N} & \text{double} \\
T_{0,1}(u): \mathbb{Z}_4 \text{ } (N \text{ odd}, \ell = 1) & \quad y_j = -\frac{1}{2} \log \tan \frac{\frac{1}{2}(j - \frac{1}{2})\pi}{N} & \text{single}
\end{aligned} \tag{6.1}$$

In each of these cases, there are no 1-strings, only *single* or *double* 2-strings at the positions given by y_j . The maximum eigenvalues in these sectors take the following real forms involving only the geometric factor $\sin 2u$

$$T_{0,0}(u) = \frac{i^{\frac{3N}{2}} e^{-Niu}}{2^{N-1}} \prod_{j=1}^{\frac{N}{2}} \left(e^{2iu} + i \tan \frac{(2j-1)\pi}{2N} \right)^2 = \frac{1}{2^{\frac{N}{2}-1}} \prod_{j=1}^{\frac{N}{2}} \left(\frac{1}{\sin \frac{(2j-1)\pi}{N}} + \sin 2u \right) \tag{6.2}$$

$$T_{0,2}(u) = \frac{Ni^{\frac{3N}{2}+1} e^{(2-N)iu}}{2^{N-1}} \prod_{j=1}^{\frac{N-2}{2}} \left(e^{2iu} + i \tan \frac{j\pi}{N} \right)^2 = \frac{N}{2^{\frac{N}{2}}} \prod_{j=1}^{\frac{N-2}{2}} \left(\frac{1}{\sin \frac{2j\pi}{N}} + \sin 2u \right) \tag{6.3}$$

$$T_{0,1}(u) = \frac{i^{\frac{3N}{2}+2} e^{-Niu}}{2^{N-1/2}} \prod_{j=1}^N \left(e^{2iu} + i \tan \frac{(2j-1)\pi}{4N} \right) = 2^{\frac{1-N}{2}} \prod_{j=1}^N \left(\frac{1}{\sin \frac{(2j-1)\pi}{2N}} + \sin 2u \right)^{\frac{1}{2}} \tag{6.4}$$

It is confirmed that these eigenvalues satisfy $T_{0,\ell}(0) = 1$ for $\ell = 0, 1, 2$.

The logarithms of the eigenvalues $T_{0,\ell}(u)$ with $\ell = 0, 1, 2$ involve sums of terms which are singular at both endpoints in the limit $N \rightarrow \infty$. To remedy this, we introduce [21] the function

$$F(t) = \log \left[t(\pi - t) \left(\frac{1}{\sin t} + \sin 2u \right) \right] = \log t + \log(\pi - t) + \log \left(\frac{1}{\sin t} + \sin 2u \right) \tag{6.5}$$

with

$$\lim_{t \rightarrow 0^+} F(t) = \lim_{t \rightarrow \pi^-} F(t) = \log \pi, \quad -\lim_{t \rightarrow 0^+} F'(t) = \lim_{t \rightarrow \pi^-} F'(t) = \frac{1}{\pi} - \sin 2u \tag{6.6}$$

For simplicity, we suppress the u dependence. The endpoint or midpoint Euler-Maclaurin formula [24] can now be applied to approximate the sum by an integral

$$\sum_{k=0}^M F(a + kh) = \frac{1}{h} \int_a^b F(t) dt + \frac{1}{2} [F(b) + F(a)] + \frac{h}{12} [F'(b) - F'(a)] + O(h^2) \tag{6.7}$$

$$\sum_{k=0}^{M-1} F(a + (k + \frac{1}{2})h) = \frac{1}{h} \int_a^b F(t) dt - \frac{h}{24} [F'(b) - F'(a)] + O(h^2) \tag{6.8}$$

where $b = a + Mh$ and h is small. Due to (6.5), we also need the asymptotic expansion of the logarithm of the gamma function

$$\log \Gamma(y) = (y - \frac{1}{2}) \log y - y + \frac{1}{2} \log(2\pi) + \frac{1}{12y} + O(y^{-2}), \quad y \rightarrow \infty \tag{6.9}$$

First, let us consider the Neveu-Schwarz sector with N even and $\ell = 2$. Setting $t_j = 2j\pi/N$, we have

$$-\log T_{0,2}(u) = \frac{N}{2} \log 2 - \log N - \sum_{j=1}^{\frac{N}{2}} F(t_j) + 2 \sum_{j=1}^{\frac{N}{2}} \log t_j \quad (6.10)$$

The sum over F can be approximated using the endpoint Euler-Maclaurin formula, with $a = 0$, $b = \pi$, $h = 2\pi/N$, and the sum over logarithms by the asymptotics of the gamma function. This yields finite-size corrections of the form (5.3) with $c = -2$ and $\Delta = \bar{\Delta} = \Delta_1 = 0$.

Next, consider the Ramond sector with $N = 0 \pmod{4}$ and $\ell = 0$. Setting $t_j = (2j-1)\pi/N$, we have

$$-\log T_{0,0}(u) = \left(\frac{N}{2} - 1\right) \log 2 - \sum_{k=0}^{\frac{N}{2}-1} F(t_j) + 2 \sum_{j=1}^{\frac{N}{2}} \log t_j \quad (6.11)$$

The sum over F can be approximated using the midpoint Euler-Maclaurin formula, with $a = 0$, $b = \pi$, $h = 2\pi/N$, and the sum over logarithms by the asymptotics of the gamma function. This yields finite-size corrections of the form (5.3) with $c = -2$ and $\Delta = \bar{\Delta} = \Delta_0 = -1/8$.

Lastly, consider the \mathbb{Z}_4 sector with N odd and $\ell = 1$. Setting $t_j = (2j-1)\pi/2N$, we have

$$-\log T_{0,1}(u) = \frac{N-1}{2} \log 2 - \frac{1}{2} \sum_{k=0}^{\frac{N}{2}-1} F(t_j) + \sum_{j=1}^{\frac{N}{2}} \log t_j \quad (6.12)$$

The sum over F can be approximated using the midpoint Euler-Maclaurin formula, with $a = 0$, $b = \pi$, $h = \pi/N$, and the sum over logarithms by the asymptotics of the gamma function. This yields finite-size corrections of the form (5.3) with $c = -2$ and $\Delta = \bar{\Delta} = \Delta_{1/2} = -3/32$.

In summary, the conformal finite-size predictions are of the expected form (5.3) with

$$c = -2, \quad \Delta = \bar{\Delta} = \Delta_{\ell/2} = -\frac{1}{8}, -\frac{3}{32}, 0, \quad \ell = 0, 1, 2 \quad (6.13)$$

The Euler-Maclaurin analysis can be extended to the excitations in these sectors as in [8] but we do not do this here. Instead, we use physical combinatorics to directly obtain the energy levels of the excited states.

7 Physical Combinatorics and Selection Rules

7.1 \mathbb{Z}_4 sectors (N odd, ℓ odd)

The building blocks of the spectra in the \mathbb{Z}_4 sectors consist of the q -binomials

$$\begin{bmatrix} n \\ m \end{bmatrix}_q = \begin{bmatrix} n \\ \lfloor n/2 \rfloor - \sigma \end{bmatrix}_q = q^{-\frac{1}{2}\sigma(\sigma+\frac{1}{2})} \sum_{\substack{\sigma\text{-single} \\ \text{columns}}} q^{\sum_j m_j E_j}, \quad \sigma = \lfloor n/2 \rfloor - m \quad (7.1)$$

with $E_j = \frac{1}{2}(j - \frac{1}{2})$. The sum is over all single-column diagrams as in Figure 13 with a fixed σ . Here σ is a quantum number given by the number of 1-strings at even positions j minus the number of 1-strings at odd positions j

$$\sigma = m_{\text{even}} - m_{\text{odd}} = \sum_{k=1}^{\lfloor n/2 \rfloor} m_{2k} - \sum_{k=1}^{\lfloor (n+1)/2 \rfloor} m_{2k-1} \quad (7.2)$$

The number of 1-strings plus 2-strings at any given position is exactly one

$$m_j + n_j = 1, \quad j = 1, 2, \dots, n \quad (7.3)$$

The single-columns with quantum number σ are generated combinatorially by starting with the minimum energy configuration of 1-strings for given σ as shown in Figure 12. Empirically determined selection rules dictate that in a sector with ℓ defects the quantum numbers of the groundstate satisfy

$$\sigma = \bar{\sigma} = \begin{cases} (\ell - 1)/4, & \ell = 1 \pmod{4} \\ -(\ell + 1)/4, & \ell = 3 \pmod{4} \end{cases} \quad \ell = |4\sigma + 1| = 1, 3, 5, 7, \dots \quad (7.4)$$

The energy of these groundstates is $E(\sigma) + E(\bar{\sigma}) = \frac{1}{16}(\ell^2 - 1)$.

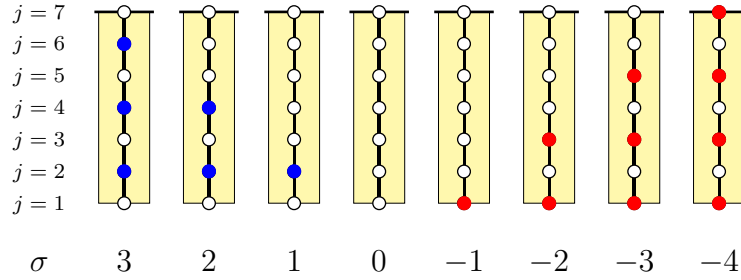


Figure 12: \mathbb{Z}_4 sectors (N, ℓ odd): Minimal configurations of single-columns with energy $E(\sigma) = \frac{1}{2}\sigma(\sigma + \frac{1}{2})$. The quantum number $\sigma = \lfloor n/2 \rfloor - m$ is given by the excess of blue (even j) over red (odd j) 1-strings. At each empty position j , there is a 2-string. This analyticity strip is in the upper-half complex u -plane rotated by 180 degrees so that position $j = 1$ (furthest from the real axis) is at the bottom.

Excitations, incrementing the energy by one unit, are generated either by inserting a pair of 1-strings at positions $j = 1$ and $j = 2$ or incrementing the position j of a 1-string by 2 units. The q -binomials are illustrated in Figure 13. Empirically, we find that all the excitations satisfy the selection rules

$$\sigma + \bar{\sigma} = \begin{cases} \frac{1}{2}(\ell - 1), & \ell = 1 \pmod{4} \\ -\frac{1}{2}(\ell + 1), & \ell = 3 \pmod{4} \end{cases} \quad \frac{1}{2}(\sigma - \bar{\sigma}) \in \mathbb{Z} \quad (7.5)$$

Using the q -binomial building blocks and empirical selection rules, we thus obtain the fini-

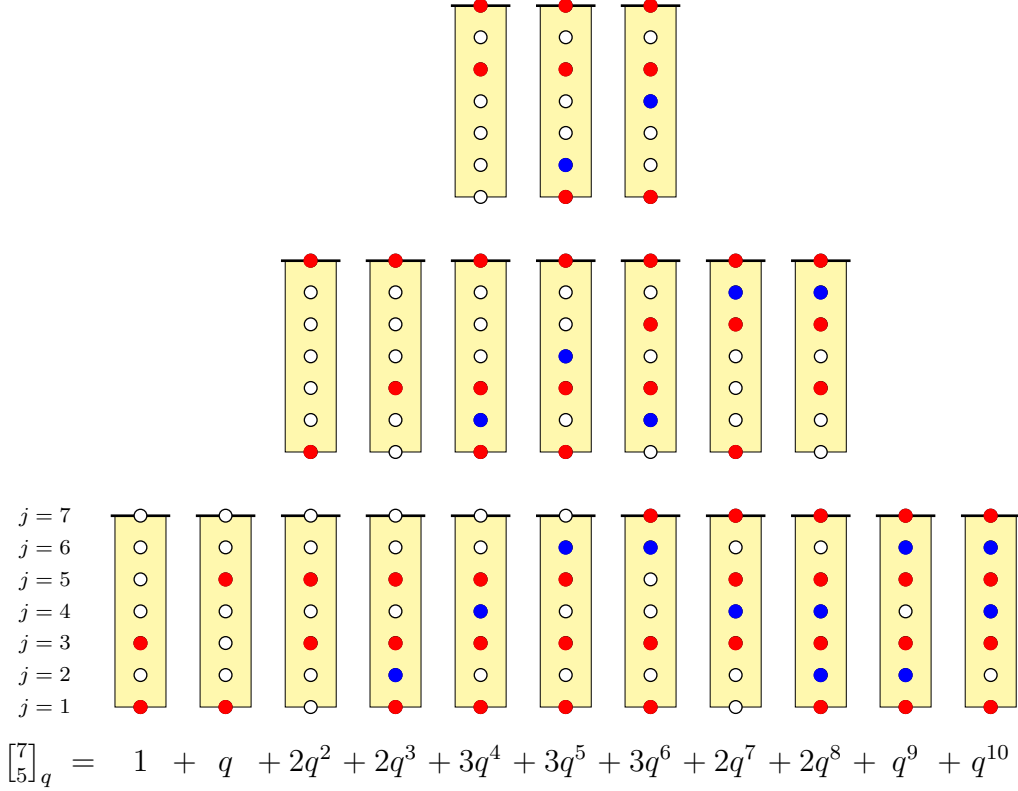


Figure 13: \mathbb{Z}_4 sectors (N, ℓ odd): Combinatorial enumeration by single-columns of the q -binomial $\begin{bmatrix} n \\ m \end{bmatrix}_q = \begin{bmatrix} 7 \\ 5 \end{bmatrix}_q = q^{-3/2} \sum q^{\sum_j m_j E_j}$. The excess of blue (even j) over red (odd j) 1-strings is given by the quantum number $\sigma = \lfloor n/2 \rfloor - m = -2$. The elementary excitation energy of a 1-string at position j is $E_j = \frac{1}{2}(j - \frac{1}{2})$. The lowest energy configuration has energy $E(\sigma) = 1/4 + 5/4 = 3/2 = \frac{1}{2}\sigma(\sigma + \frac{1}{2})$. At each empty position j , there is a 2-string. This analyticity strip is in the upper-half complex u -plane rotated by 180 degrees so that position $j = 1$ (furthest from the real axis) is at the bottom. The elementary excitations (of energy 1) are generated by either inserting two 1-strings at positions $j = 1$ and $j = 2$ or promoting a 1-string at position j to position $j + 2$. Notice that $\begin{bmatrix} n \\ m \end{bmatrix}_q = \begin{bmatrix} n \\ n-m \end{bmatrix}_q$ as q -polynomials but they have different combinatorial interpretations because they have different quantum numbers σ . In the lower half-plane, q is replaced with \bar{q} and no rotation is required. In this example, $\ell = 7$ and the value $\bar{\sigma} = -2$ of the quantum number in the lower half-plane is related to $\sigma = -2$ in the upper half-plane by the selection rules $\sigma + \bar{\sigma} = -(\ell + 1)/2$ and $\frac{1}{2}(\sigma - \bar{\sigma}) \in \mathbb{Z}$.

tized partition functions

$$Z_\ell^{(N)}(q) = \begin{cases} (q\bar{q})^{-c/24} \sum_{k \in \mathbb{Z}} q^{\Delta_{2k+\ell/2}} \begin{bmatrix} \frac{N+1}{2} \\ \frac{N-\ell}{4} - k \end{bmatrix}_q \bar{q}^{\Delta_{2k-\ell/2}} \begin{bmatrix} \frac{N-1}{2} \\ \frac{N-\ell}{4} + k \end{bmatrix}_{\bar{q}} \\ (q\bar{q})^{-c/24} \sum_{k \in \mathbb{Z}} q^{\Delta_{2k+\ell/2}} \begin{bmatrix} \frac{N+1}{2} \\ \frac{N+\ell+2}{4} + k \end{bmatrix}_q \bar{q}^{\Delta_{2k-\ell/2}} \begin{bmatrix} \frac{N-1}{2} \\ \frac{N+\ell-2}{4} - k \end{bmatrix}_{\bar{q}} \end{cases} \quad N-\ell = 0 \pmod{4} \quad (7.6)$$

$$Z_\ell^{(N)}(q) = \begin{cases} (q\bar{q})^{-c/24} \sum_{k \in \mathbb{Z}} q^{\Delta_{2k+\ell/2}} \begin{bmatrix} \frac{N+1}{2} \\ \frac{N-\ell+2}{4} - k \end{bmatrix}_q \bar{q}^{\Delta_{2k-\ell/2}} \begin{bmatrix} \frac{N-1}{2} \\ \frac{N-\ell-2}{4} + k \end{bmatrix}_{\bar{q}} \\ (q\bar{q})^{-c/24} \sum_{k \in \mathbb{Z}} q^{\Delta_{2k+\ell/2}} \begin{bmatrix} \frac{N+1}{2} \\ \frac{N+\ell}{4} + k \end{bmatrix}_q \bar{q}^{\Delta_{2k-\ell/2}} \begin{bmatrix} \frac{N-1}{2} \\ \frac{N+\ell}{4} - k \end{bmatrix}_{\bar{q}} \end{cases} \quad N-\ell = 2 \pmod{4} \quad (7.7)$$

For given mod 4 parities of $N - \ell$, these expressions are equivalent as partition functions but, in each case, the first form is used for the combinatorial interpretation when $\ell = 1 \pmod{4}$ and the second form when $\ell = 3 \pmod{4}$. We further observe that

$$\sum_{\ell \in 2\mathbb{N}-1}^{\ell \leq N} Z_\ell^{(N)}(q) = \frac{1}{2} (q\bar{q})^{-\frac{c}{24} - \frac{3}{32}} \left[\prod_{n=1}^{\frac{N+1}{2}} (1 + q^{\frac{2n-1}{4}}) \prod_{n=1}^{\frac{N-1}{2}} (1 + \bar{q}^{\frac{2n-1}{4}}) + \prod_{n=1}^{\frac{N+1}{2}} (1 - q^{\frac{2n-1}{4}}) \prod_{n=1}^{\frac{N-1}{2}} (1 - \bar{q}^{\frac{2n-1}{4}}) \right] \quad (7.8)$$

7.2 Ramond sectors (N even, $\ell/2$ even)

The building blocks of the spectra in the Ramond sectors consist of the q -binomials

$$\begin{bmatrix} n \\ m \end{bmatrix}_q = \begin{bmatrix} n \\ \lfloor n/2 \rfloor - \sigma \end{bmatrix}_q = q^{-\frac{1}{2}\sigma^2} \sum_{\substack{\sigma\text{-double} \\ \text{columns}}} q^{\sum_j m_j E_j}, \quad \sigma = \lfloor n/2 \rfloor - m \quad (7.9)$$

with $E_j = j - \frac{1}{2}$. The sum is over all double-column diagrams as in Figure 15 with a fixed σ . Here σ is a quantum number given by the number of 1-strings in the right column minus the number of 1-strings in the left column

$$\sigma = m_{\text{right}} - m_{\text{left}} \quad (7.10)$$

The number of 1-strings plus 2-strings at any given position is exactly two

$$m_j + n_j = 2, \quad j = 1, 2, \dots, n \quad (7.11)$$

The double-columns with quantum number σ are generated combinatorially by starting with the minimum energy configuration of 1-strings for given σ as shown in Figure 14. Empirically determined selection rules dictate that in a sector with ℓ defects the quantum numbers of the groundstate satisfy

$$\sigma = \bar{\sigma} = \ell/4, \quad \ell = 0, 4, 8, \dots \quad (7.12)$$

The energy of these groundstates is $E(\sigma) + E(\bar{\sigma}) = \frac{1}{16} \ell^2$.

Excitations, incrementing the energy by one unit, are generated either by inserting a left-right pair of 1-strings at position $j = 1$ or incrementing the position j of a 1-string

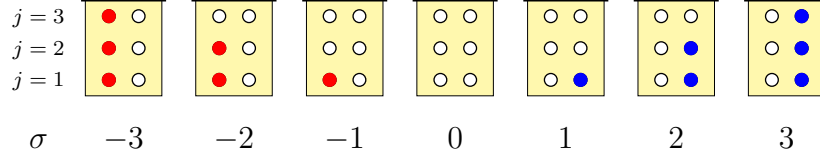


Figure 14: Ramond sectors (N even, $\ell/2$ even): Minimal configurations of double-columns with energy $E(\sigma) = \frac{1}{2}\sigma^2$. The quantum number $\sigma = \lfloor n/2 \rfloor - m$ is given by the excess of blue (right) over red (left) 1-strings. At each position j , the number of 1-strings m_j plus the number of 2-strings n_j is 2. This analyticity strip is in the upper-half complex u -plane rotated by 180 degrees so that position $j = 1$ (furthest from the real axis) is at the bottom.

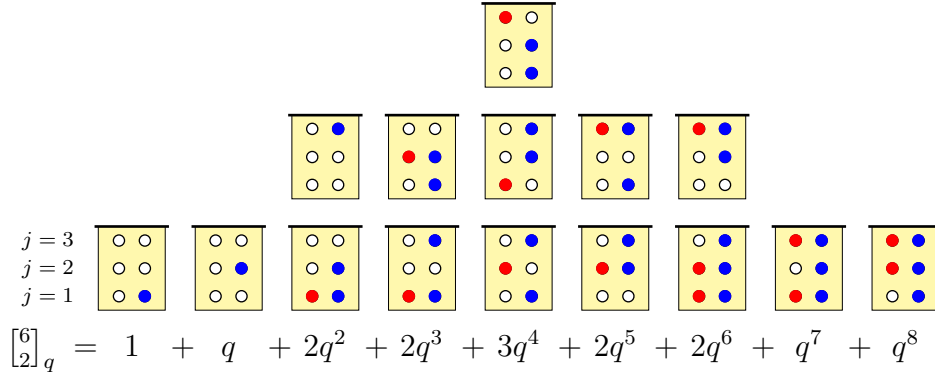


Figure 15: Ramond sectors (N even, $\ell/2$ even): Combinatorial enumeration by double-columns of the q -binomial $\begin{bmatrix} n \\ m \end{bmatrix}_q = \begin{bmatrix} 6 \\ 2 \end{bmatrix}_q = q^{-1/2} \sum q^{\sum_j m_j E_j}$. The excess of blue (right) over red (left) 1-strings is given by the quantum number $\sigma = \lfloor n/2 \rfloor - m = 1$. The elementary excitation energy of a 1-string at position j is $E_j = j - \frac{1}{2}$. The lowest energy configuration has energy $E(\sigma) = \frac{1}{2}\sigma^2 = \frac{1}{2}$. At each position j , there are m_j 1-strings and $n_j = 2 - m_j$ 2-strings. This analyticity strip is in the upper-half complex u -plane rotated by 180 degrees so that position $j = 1$ (furthest from the real axis) is at the bottom. The elementary excitations (of energy 1) are generated by either inserting a left-right pair of 1-strings at position $j = 1$ or promoting a 1-string at position j to position $j + 1$. Notice that $\begin{bmatrix} n \\ m \end{bmatrix}_q = \begin{bmatrix} n \\ n-m \end{bmatrix}_q$ as q -polynomials but they have different combinatorial interpretations because they have different quantum numbers σ . In the lower half-plane, q is replaced with \bar{q} and no rotation is required. The value $\bar{\sigma}$ of the quantum number in the lower half-plane is related to σ in the upper half-plane by the selection rules $\sigma + \bar{\sigma} = \ell/2$ and $\frac{1}{2}(\sigma - \bar{\sigma}) \in \mathbb{Z}$.

by 1 unit. The q -binomials are illustrated in Figure 15. Empirically, we find that all the excitations satisfy the selection rules

$$\sigma + \bar{\sigma} = \ell/2, \quad \frac{1}{2}(\sigma - \bar{\sigma}) \in \mathbb{Z} \quad (7.13)$$

Using the q -binomial building blocks and empirical selection rules, we thus obtain the finitized partition functions

$$Z_\ell^{(N)}(q) = (q\bar{q})^{-c/24} \sum_{k \in \mathbb{Z}} q^{\Delta_{2k+\ell/2}} \begin{bmatrix} 2\lfloor \frac{N+2}{4} \rfloor \\ \lfloor \frac{N+2-\ell}{4} \rfloor - k \end{bmatrix}_q \bar{q}^{\Delta_{2k-\ell/2}} \begin{bmatrix} 2\lfloor \frac{N}{4} \rfloor \\ \lfloor \frac{N-\ell}{4} \rfloor + k \end{bmatrix}_{\bar{q}}, \quad N \text{ even, } \frac{\ell}{2} \text{ even} \quad (7.14)$$

We further observe that

$$\begin{aligned} Z_0^{(N)} + 2 \sum_{\ell \in 4\mathbb{N}}^{\ell \leq N} Z_\ell^{(N)}(q) &= \frac{1}{2} (q\bar{q})^{-\frac{c}{24} - \frac{1}{8}} \left[\prod_{n=1}^{\lfloor \frac{N+2}{4} \rfloor} (1 + q^{n-\frac{1}{2}})^2 \prod_{n=1}^{\lfloor \frac{N}{4} \rfloor} (1 + \bar{q}^{n-\frac{1}{2}})^2 \right. \\ &\quad \left. + \prod_{n=1}^{\lfloor \frac{N+2}{4} \rfloor} (1 - q^{n-\frac{1}{2}})^2 \prod_{n=1}^{\lfloor \frac{N}{4} \rfloor} (1 - \bar{q}^{n-\frac{1}{2}})^2 \right] \end{aligned} \quad (7.15)$$

7.3 Neveu-Schwarz sectors (N even, $\ell/2$ odd)

The building blocks of the spectra in the Neveu-Schwarz sectors consist of the q -binomials

$$\begin{bmatrix} n \\ m \end{bmatrix}_q = \begin{bmatrix} n \\ \lfloor n/2 \rfloor - \sigma \end{bmatrix}_q = q^{-\frac{1}{2}\sigma(\sigma+1)} \sum_{\substack{\sigma\text{-double} \\ \text{columns}}} q^{\sum_j m_j E_j}, \quad \sigma = \lfloor n/2 \rfloor - m \quad (7.16)$$

with $E_j = j$. The sum is over all double-column diagrams as in Figure 17 with fixed σ . In these sectors, the number of 1-strings in the right column minus the number of 1-strings in the left column is related to the quantum number σ by

$$m_{\text{right}} - m_{\text{left}} = \sigma \quad \text{or} \quad \sigma + 1 \quad (7.17)$$

The number of 1-strings plus 2-strings at any given position is exactly two

$$m_j + n_j = 2, \quad j = 1, 2, \dots, n \quad (7.18)$$

The double-columns with quantum number σ are generated combinatorially by starting with the minimum energy configuration of 1-strings for given σ as shown in Figure 16. For these *minimum* energy configurations

$$m_{\text{right}} - m_{\text{left}} = \sigma_{\min} = \begin{cases} \sigma, & \sigma \geq 0 \\ \sigma + 1, & \sigma < 0 \end{cases} \quad (7.19)$$

Empirically determined selection rules dictate that in a sector with ℓ defects the quantum numbers of the groundstate satisfy

$$\sigma = \bar{\sigma} = (\ell - 2)/4, \quad \ell = 2, 6, 10, \dots \quad (7.20)$$

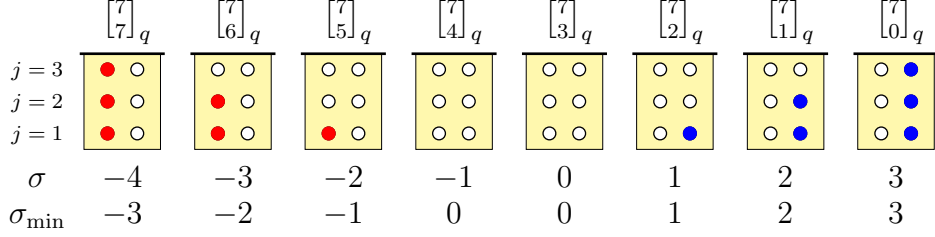
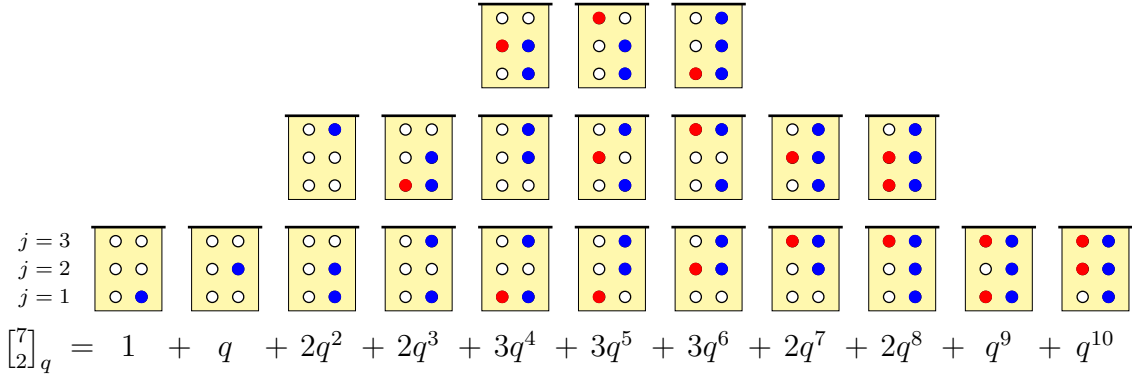


Figure 16: Neveu-Schwarz sectors (N even, $\ell/2$ odd): Minimal configurations of double-columns within the binomials $\begin{bmatrix} n \\ m \end{bmatrix}_q = \begin{bmatrix} 7 \\ m \end{bmatrix}_q$. The energy is $E(\sigma) = \frac{1}{2}\sigma(\sigma + 1)$ where the quantum number is $\sigma = \lfloor n/2 \rfloor - m$. The excess of blue (right) over red (left) 1-strings in these minimal configurations is σ_{\min} as given in (7.19). At each position j , the number of 1-strings m_j plus the number of 2-strings n_j is 2. This analyticity strip is in the upper-half complex u -plane rotated by 180 degrees so that position $j = 1$ (furthest from the real axis) is at the bottom.



The energy of these groundstates is $E(\sigma) + E(\bar{\sigma}) = \frac{1}{16}(\ell^2 - 4)$.

Excitations, incrementing the energy by one unit, are generated either by inserting a left or right 1-string at position $j = 1$ or incrementing the position j of a 1-string by 1 unit. The q -binomials are illustrated in Figure 17. Empirically, we find that all the excitations are consistent with the selection rules

$$\sigma + \bar{\sigma} = (\ell - 2)/2, \quad \frac{1}{2}(\sigma - \bar{\sigma}) \in \mathbb{Z} \quad (7.21)$$

Using the q -binomial building blocks and empirical selection rules, we thus obtain the finitized partition functions

$$Z_\ell^{(N)}(q) = (q\bar{q})^{-c/24} \sum_{k \in \mathbb{Z}} q^{\Delta_{2k+\ell/2}} \begin{bmatrix} 2\lfloor \frac{N}{4} \rfloor + 1 \\ \lfloor \frac{N+2-\ell}{4} \rfloor - k \end{bmatrix}_q \bar{q}^{\Delta_{2k-\ell/2}} \begin{bmatrix} 2\lfloor \frac{N+2}{4} \rfloor - 1 \\ \lfloor \frac{N-\ell}{4} \rfloor + k \end{bmatrix}_{\bar{q}}, \quad N \text{ even, } \frac{\ell}{2} \text{ odd} \quad (7.22)$$

We further observe that

$$\sum_{\ell \in 4\mathbb{N}-2}^{\ell \leq N} Z_\ell^{(N)}(q) = (q\bar{q})^{-\frac{c}{24}} \prod_{n=1}^{\lfloor \frac{N}{4} \rfloor} (1 + q^n)^2 \prod_{n=1}^{\lfloor \frac{N-2}{4} \rfloor} (1 + \bar{q}^n)^2 \quad (7.23)$$

7.4 Finitized characters in Ramond and Neveu-Schwarz sectors

In the Ramond and Neveu-Schwarz sectors with N even, the q -binomials do not give the appropriate characters. In fact, the relevant finitized irreducible characters are given [8, 25] by the generalized q -Catalan numbers

$$\text{ch}_{r,1}^{(n)}(q) = q^{-\frac{c}{24}} \sum_{m=0}^{\frac{n-2r}{2}} \left\langle m, m+r-1 \right\rangle_q = q^{-\frac{c}{24} + \Delta_{r,1}} \frac{1 - q^r}{1 - q^{n/2}} \begin{bmatrix} n \\ \frac{n}{2} - r \end{bmatrix}_q, \quad n \text{ even} \quad (7.24)$$

$$\text{ch}_{r,2}^{(n)}(q) = q^{-\frac{c}{24} - \frac{4r-3}{8}} \sum_{m=0}^{\frac{n-2r+1}{2}} q^{-m} \left\langle m, m+r-1 \right\rangle_q = q^{-\frac{c}{24} + \Delta_{r,2}} \frac{1 - q^{2r}}{1 - q^{n+1}} \begin{bmatrix} n+1 \\ \frac{n+1}{2} - r \end{bmatrix}_q, \quad n \text{ odd} \quad (7.25)$$

Here

$$\left\langle \begin{matrix} M \\ m, n \end{matrix} \right\rangle_q = q^{\frac{1}{2}m(m+1) + \frac{1}{2}n(n+1)} \left(\begin{bmatrix} M \\ m \end{bmatrix}_q \begin{bmatrix} M \\ n \end{bmatrix}_q - q^{n-m+1} \begin{bmatrix} M \\ n+1 \end{bmatrix}_q \begin{bmatrix} M \\ m-1 \end{bmatrix}_q \right) \quad (7.26)$$

are generalized versions [8] of the q -Narayana numbers [26] and the generalized Catalan numbers are

$$\text{ch}_{r,1}^{(n)}(1) = \binom{n-2}{\frac{n-2}{2} - r + 1} - \binom{n-2}{\frac{n-2}{2} - r - 1}, \quad r \geq 1, n \text{ even} \quad (7.27)$$

$$\text{ch}_{r,2}^{(n)}(1) = \binom{n-1}{\frac{n-1}{2} - r + 1} - \binom{n-1}{\frac{n-1}{2} - r - 1}, \quad r \geq 1, n \text{ odd} \quad (7.28)$$

Despite the minus sign, (7.26) is actually a polynomial with only non-negative coefficients. Combinatorially, the generalized q -Narayana numbers are generated by double-column diagrams subject to admissibility (dominance) as shown in Figure 18.

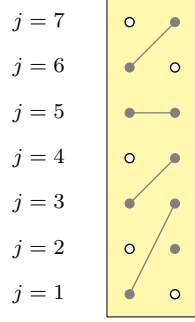


Figure 18: An admissible double-column diagram with $m = 4$ and $n = 5$ satisfying dominance $L = \{6, 5, 3, 1\} \preceq \{7, 5, 4, 3, 2\} = R$. The energy is $E = 15 + 21 = 36$ and the associated monomial is q^{36} .

A *double-column configuration* of height M consists of a pair of single-column configurations of height M . Suppose that there are m occupied heights in the left column and n occupied heights in the right column with $0 \leq m \leq n \leq M$. Let $L = \{L_1, L_2, \dots, L_m\}$ be the occupied heights j in descending order of the left column and $R = \{R_1, R_2, \dots, R_n\}$ be the occupied heights j in descending order of the right column. We say the double-column diagram is admissible or satisfies dominance if $L \preceq R$ with the partial order

$$L \preceq R \quad \iff \quad L_k \leq R_k, \quad j = 1, 2, \dots, m \quad (7.29)$$

Geometrically, one draws line segments between the occupied sites of greatest height in the two columns, then between the occupied sites of second-to-greatest height, and so on. Admissible double-column configurations are now characterized by *not* involving line segments with a *strictly negative slope*.

We associate the monomial q^E to each double-column configuration where

$$E = \sum_{k=1}^m L_k + \sum_{k=1}^n R_k \quad (7.30)$$

is the energy or weight of a double-column configuration. The generalized q -Narayana number

$$\left\langle \begin{matrix} M \\ m, n \end{matrix} \right\rangle_q = \sum_{\substack{\text{admissible} \\ \text{double-columns}}} q^E \quad (7.31)$$

is the sum of the monomials associated to the admissible double-column diagrams of height M and occupancy m and n in the left and right columns, respectively.

The q -binomials decompose in terms of finitized irreducible characters

$$q^{-\frac{c}{24} + \Delta_{r,1}} \left[\begin{matrix} 2n+1 \\ n-r-1 \end{matrix} \right]_q = \sum_{t=r}^{n+1} \text{ch}_{t,1}^{(2n+2)}(q) \quad (7.32)$$

$$q^{-\frac{c}{24} + \Delta_{r,2}} \left[\begin{matrix} 2n \\ n-r+1 \end{matrix} \right]_q = \sum_{t=r, \text{ by } 2}^{n \text{ or } n+1} \text{ch}_{t,2}^{(2n+1)}(q) \quad (7.33)$$

Substituting the decompositions (7.32) and (7.33) into (7.14) and (7.22), we obtain the finitized partition functions

$$Z_\ell^{(N)}(q) = \begin{cases} \sum_{r=1}^{\lfloor \frac{N+6}{4} \rfloor} \sum_{\bar{r}=1}^{\lfloor \frac{N+4}{4} \rfloor} Z_{\ell,r,\bar{r}} \text{ch}_{r,2}^{(2\lfloor \frac{N+2}{4} \rfloor+1)}(q) \text{ch}_{\bar{r},2}^{(2\lfloor \frac{N}{4} \rfloor+1)}(\bar{q}), & \frac{\ell}{2} \text{ even} \\ \sum_{r=1}^{\lfloor \frac{N+4}{4} \rfloor} \sum_{\bar{r}=1}^{\lfloor \frac{N+2}{4} \rfloor} Z_{\ell,r,\bar{r}} \text{ch}_{r,1}^{(2\lfloor \frac{N}{4} \rfloor+2)}(q) \text{ch}_{\bar{r},1}^{(2\lfloor \frac{N+2}{4} \rfloor)}(\bar{q}), & \frac{\ell}{2} \text{ odd} \end{cases} \quad (7.34)$$

where the coefficients $Z_{\ell,r,\bar{r}}$ are given by

$$Z_{\ell,r,\bar{r}} = \begin{cases} \frac{1}{4}(1 + (-1)^{r+\bar{r}}) [\max(\frac{\ell}{2}, r + \bar{r}) - \max(\frac{\ell}{2}, |r - \bar{r}|)], & \frac{\ell}{2} \text{ even} \\ \max(\frac{\ell}{2}, r + \bar{r}) - \max(\frac{\ell}{2}, |r - \bar{r}|), & \frac{\ell}{2} \text{ odd} \end{cases} \quad (7.35)$$

8 Conformal Partition Functions

As $N \rightarrow \infty$, the finitized characters become conformal characters. From (7.6), (7.7) and (7.34), the conformal partition functions are given by the sesquilinear forms

$$Z_\ell(q) = \begin{cases} \sum_{k=-\infty}^{\infty} \text{ch}_{2k+\ell/2}(q) \text{ch}_{2k-\ell/2}(\bar{q}), & \mathbb{Z}_4 \ (\ell \text{ odd}) \\ \sum_{r,\bar{r}=1}^{\infty} Z_{\ell,r,\bar{r}} \text{ch}_{r,2}(q) \text{ch}_{\bar{r},2}(\bar{q}), & \text{Ramond} \ (\frac{\ell}{2} \text{ even}) \\ \sum_{r,\bar{r}=1}^{\infty} Z_{\ell,r,\bar{r}} \text{ch}_{r,1}(q) \text{ch}_{\bar{r},1}(\bar{q}), & \text{Neveu-Schwarz} \ (\frac{\ell}{2} \text{ odd}) \end{cases} \quad (8.1)$$

Summing over sectors with either $\ell/2$ even or $\ell/2$ odd, we find

$$\sum_{\ell} Z_{\ell,r,\bar{r}} = \begin{cases} Z_{r,\bar{r}} = \frac{1}{4} [1 + (-1)^{r+\bar{r}}] [\binom{r+1}{2} + \binom{\bar{r}+1}{2} - \binom{|r-\bar{r}|+1}{2}], & \frac{\ell}{2} \text{ even} \\ r \bar{r}, & \frac{\ell}{2} \text{ odd} \end{cases} \quad (8.2)$$

and hence

$$Z(q) = \begin{cases} \sum_{\ell \in 2\mathbb{N}-1} \sum_{k=-\infty}^{\infty} \text{ch}_{2k+\ell/2}(q) \text{ch}_{2k-\ell/2}(\bar{q}), & \mathbb{Z}_4 \ (\ell \text{ odd}) \\ \sum_{r,\bar{r}=1}^{\infty} Z_{r,\bar{r}} \text{ch}_{r,2}(q) \text{ch}_{\bar{r},2}(\bar{q}), & \text{Ramond} \ (\frac{\ell}{2} \text{ even}) \\ \sum_{r,\bar{r}=1}^{\infty} r \bar{r} \text{ch}_{r,1}(q) \text{ch}_{\bar{r},1}(\bar{q}), & \text{Neveu-Schwarz} \ (\frac{\ell}{2} \text{ odd}) \end{cases} \quad (8.3)$$

Let us define the theta functions

$$\vartheta_{s,p}(q) = \sum_{\lambda \in \mathbb{Z} + \frac{s}{2p}} q^{p\lambda^2} \quad (8.4)$$

It follows from (7.6) and (7.7), after summing over the \mathbb{Z}_4 sectors, that

$$\sum_{\ell \in 2\mathbb{N}-1} Z_\ell(q) = \frac{|\vartheta_{\frac{1}{2},2}(q)|^2 + |\vartheta_{\frac{3}{2},2}(q)|^2}{|\eta(q)|^2} \quad (8.5)$$

where the Dedekind eta function is

$$\eta(q) = q^{1/24} \prod_{n=1}^{\infty} (1 - q^n) \quad (8.6)$$

Similarly, from (7.14) and (7.22), we note that summing over the ℓ even sectors with suitable multiplicities yields

$$\begin{aligned} Z_0(q) + 2 \sum_{\ell \in 4\mathbb{N}} Z_\ell(q) &= \frac{|\vartheta_{0,2}(q)|^2 + |\vartheta_{2,2}(q)|^2}{|\eta(q)|^2} = |\hat{\chi}_{-1/8}(q)|^2 + |\hat{\chi}_{3/8}(q)|^2 \\ 2 \sum_{\ell \in 4\mathbb{N}-2} Z_\ell(q) &= \frac{|\vartheta_{1,2}(q)|^2 + |\vartheta_{3,2}(q)|^2}{|\eta(q)|^2} = \frac{2|\vartheta_{1,2}(q)|^2}{|\eta(q)|^2} = 2|\hat{\chi}_0(q) + \hat{\chi}_1(q)|^2 \\ Z_0(q) + 2 \sum_{\ell \in 2\mathbb{N}} Z_\ell(q) &= \frac{1}{|\eta(q)|^2} \sum_{s=0}^3 |\vartheta_{s,2}(q)|^2 = |\hat{\chi}_{-1/8}(q)|^2 + |\hat{\chi}_{3/8}(q)|^2 + 2|\hat{\chi}_0(q) + \hat{\chi}_1(q)|^2 \end{aligned} \quad (8.7)$$

where the \mathcal{W} -irreducible characters are

$$\begin{aligned} \hat{\chi}_{-1/8}(q) &= \frac{1}{\eta(q)} \vartheta_{0,2}(q), & \hat{\chi}_0(q) &= \frac{1}{2\eta(q)} [\vartheta_{1,2}(q) + \eta(q)^3] \\ \hat{\chi}_{3/8}(q) &= \frac{1}{\eta(q)} \vartheta_{2,2}(q), & \hat{\chi}_1(q) &= \frac{1}{2\eta(q)} [\vartheta_{1,2}(q) - \eta(q)^3] \end{aligned} \quad (8.8)$$

In the last equation of (8.7), we have produced a modular invariant which we believe is the correct modular invariant partition function for critical dense polymers on the torus. However, we stress that this partition function is not obtained by the naive trace summing over all even N sectors since we have changed the multiplicity of all of the $\ell \neq 0$ sectors by a factor of 2. We note that the naive trace does not yield a modular invariant.

Although we do not give details, the methods of this paper also apply to the case of Identified Connectivities (IC) so we include the results for completeness. In this case there are no defects, $E_j = j$ and the finitized partition function is

$$Z_{IC}^{(N)}(q) = \sum_{r=1}^{\lfloor \frac{N}{4} \rfloor} \text{ch}_{r,1}^{(2\lfloor \frac{N}{4} \rfloor)}(q) \text{ch}_{r,1}^{(2\lfloor \frac{N-2}{4} \rfloor)}(\bar{q}) \quad (8.9)$$

It follows that the conformal partition function is

$$Z_{IC}(q) = \sum_{r=1}^{\infty} |\text{ch}_{r,1}(q)|^2 \quad (8.10)$$

Further results could be obtained for the case of Distinguished Connectivities (DC) with ℓ defects and $\alpha = 0$ or $\alpha = -2$. The cases $\alpha \neq 0, \pm 2$ are also integrable but can not be solved in the $\ell = 0$ sector by the simple factorization techniques used in this paper.

9 Conclusion

In this paper, we have solved a model of critical dense polymers exactly on arbitrary finite-size cylinders. This topology allows for non-contractible loops with fugacity α that wind around the cylinder or for an arbitrary number ℓ of defects that propagate along the full length of the cylinder. We have set up commuting transfer matrices that satisfy a functional equation in the form of an inversion identity. For even N with loop fugacity $\alpha = 2$, this involves a non-diagonalizable braid operator \mathbf{J} and an involution $\mathbf{R} = -(\mathbf{J}^3 - 12\mathbf{J})/16 = (-1)^{\mathbf{F}}$ with eigenvalues $R = (-1)^{\ell/2}$. This is reminiscent of supersymmetry with a pair of defects interpreted as a fermion and \mathbf{F} as a fermi number operator. However, we have no direct evidence of fermions or supersymmetry in our model. Nevertheless, since the number of defects ℓ is a quantum number that separates the theory into various sectors, we call these sectors Ramond ($\ell/2$ even), Neveu-Schwarz ($\ell/2$ odd) and \mathbb{Z}_4 (ℓ odd), respectively. We conjecture that, when acting on link states with an arbitrary even number of defects, the braid operator \mathbf{R} and transfer matrices $\mathbf{T}(u)$ are of rank 2 and have no rank-3 or higher Jordan blocks for arbitrary even N . The existence of non-trivial Jordan blocks is indicative that the theory on a long cylinder or torus is logarithmic in the sense that it gives rise to indecomposable representations of the Virasoro generator L_0 .

For $\alpha = 2$ and arbitrary N , the inversion identity is solved exactly sector by sector for the eigenvalues of the transfer matrices in finite geometry. We thus obtain finitized conformal partition functions as sesquilinear forms in appropriate finitized characters. The eigenvalues are classified by the physical combinatorics of the patterns of zeros in the complex spectral-parameter plane. This yields selection rules for the physically relevant solutions to the inversion identity. The finite-size corrections follow from Euler-Maclaurin formulas. In the scaling limit, we obtain the conformal partition functions as sesquilinear forms and confirm [2, 3, 4] the central charge $c = -2$ and conformal weights $\Delta, \bar{\Delta} = \Delta_t = (t^2 - 1)/8$. Here $t = \ell/2$ and $t = 2r - s \in \mathbb{N}$ in the ℓ even sectors with Kac labels $r = 1, 2, 3, \dots; s = 1, 2$ while $t \in \mathbb{Z} - \frac{1}{2}$ in the ℓ odd sectors. Strikingly, the $\ell/2$ odd sectors exhibit a \mathcal{W} -extended symmetry but the $\ell/2$ even sectors do not. Moreover, the naive trace summing over all even N sectors does not yield a modular invariant.

Recently, we considered [14] critical dense polymers on the strip with boundary conditions that, in the continuum scaling limit, respect a \mathcal{W} -extended symmetry. Our analysis enabled us to identify this model with the $c_{1,2}$ triplet model or symplectic fermions on the strip. It appears that no such simple identification can be made between these models on a long cylinder or torus after taking a naive trace. To resolve this seeming paradox, it may be necessary to modify the lattice model on a cylinder to properly restore the fermion structure and supersymmetry, or to introduce a modified trace implementing the proper torus geometry. Only then can we hope to have a proper interpretation of the fermi number operator \mathbf{F} and find agreement, in the N even sectors, with the conformal partition functions obtained by Saleur [4]. We intend to return to this question in a later publication.

Acknowledgments

This work is supported by the Australian Research Council.

A Properties of \mathbf{J}

For N even, \mathbf{J} contains a non-contractible loop in exactly two diagrams

$$\mathbf{J} = \mathbf{J}_0 + \mathbf{J}_1 \quad (\text{A.1})$$

where \mathbf{J}_0 refers to the part without non-contractible loops, while

$$(-1)^{\frac{N}{2}} \mathbf{J}_1 = \begin{array}{|c|c|c|c|c|c|c|c|} \hline \text{Diagram 1} \\ \hline \end{array} + \begin{array}{|c|c|c|c|c|c|c|c|} \hline \text{Diagram 2} \\ \hline \end{array} \quad (\text{A.2})$$

(here illustrated for $N = 8$). In the enlarged TL algebra, this is just $\alpha\Omega(E + F)$.

In order to describe \mathbf{J} , and not just \mathbf{J}_1 , in terms of the enlarged TL algebra, we introduce the ‘periodically ordered subsets’ $\bar{\sigma}_n$ defined as follows. For $n < N$, let $\{\sigma_1, \dots, \sigma_n\}$ be a set of distinct elements of $\{0, \dots, N-1\}$, and let $\bar{\sigma}_n$ be an ordering of $\{\sigma_1, \dots, \sigma_n\}$ for which $\sigma_{j+1} \neq \sigma_j - 1$ and $\sigma_1 \neq \sigma_n - 1$. Two such orderings are equivalent if the corresponding ordered products of periodic TL generators match

$$\bar{\sigma}_n \sim \bar{\sigma}'_n \Leftrightarrow e_{\sigma_1} \dots e_{\sigma_n} = e_{\sigma'_1} \dots e_{\sigma'_n} \quad (\text{A.3})$$

We can now write \mathbf{J} in terms of the enlarged TL algebra as

$$\begin{aligned} \mathbf{J} &= (-1)^N \Omega^2 + \sum_{n=1}^{N-1} (-1)^{N-n} \sum_{[\bar{\sigma}_n]} (e_{\sigma_1} \dots e_{\sigma_n} \Omega)^2 + \Omega^{-2} \\ &= (-1)^N \Omega^2 + \sum_{n=1}^{N-1} (-1)^{N-n} \sum_{[\bar{\sigma}_n]} (\Omega e_{\sigma_1} \dots e_{\sigma_n})^2 + \Omega^{-2} \\ &= (-1)^N \Omega^2 + \sum_{n=1}^{N-1} (-1)^{N-n} \sum_{[\bar{\sigma}_n]} (e_{\sigma_n} \dots e_{\sigma_1} \Omega^{-1})^2 + \Omega^{-2} \\ &= (-1)^N \Omega^2 + \sum_{n=1}^{N-1} (-1)^{N-n} \sum_{[\bar{\sigma}_n]} (\Omega^{-1} e_{\sigma_n} \dots e_{\sigma_1})^2 + \Omega^{-2} \end{aligned} \quad (\text{A.4})$$

where the sum $\sum_{[\bar{\sigma}_n]}$ is over the set of equivalence classes of periodically ordered subsets of cardinality n . $\bar{\sigma}_n$ is thus a representative of the given equivalence class.

A.1 Proof of Inversion Identity

Proof of Inversion Identity (Section 4.1) Recalling that $\lambda = \frac{\pi}{2}$, the left side of (4.5) corresponds diagrammatically to

$$\mathbf{T}(u)\mathbf{T}(u + \frac{\pi}{2}) = \begin{array}{|c|c|c|c|c|c|c|} \hline u+\lambda & & \dots & & & \dots & & u+\lambda \\ \hline u & & \dots & & & \dots & & u \\ \hline \end{array} \quad (\text{A.5})$$

with the left and right (vertical) edges identified. First, we examine the consequences of

having a half-arc connecting the two left nodes (or two right nodes) of a 3-tangle (two-column) appearing in (A.5). Expanding in terms of connectivities, we find

$$\begin{array}{c} u+\lambda \\ \hline u \end{array} = -\sin u \cos u \begin{array}{c} \text{diag 1} \\ \text{diag 2} \end{array} + \cos u \sin u \begin{array}{c} \text{diag 3} \\ \text{diag 4} \end{array} - \sin^2 u \begin{array}{c} \text{diag 5} \\ \text{diag 6} \end{array} + 0 \begin{array}{c} \text{diag 7} \\ \text{diag 8} \end{array} = -\sin^2 u \begin{array}{c} \text{diag 9} \\ \text{diag 10} \end{array} \quad (\text{A.6})$$

$$\begin{array}{c} u+\lambda \\ \hline u \end{array} = -\sin u \cos u \begin{array}{c} \text{diag 11} \\ \text{diag 12} \end{array} + \cos u \sin u \begin{array}{c} \text{diag 13} \\ \text{diag 14} \end{array} + 0 \begin{array}{c} \text{diag 15} \\ \text{diag 16} \end{array} + \cos^2 u \begin{array}{c} \text{diag 17} \\ \text{diag 18} \end{array} = \cos^2 u \begin{array}{c} \text{diag 19} \\ \text{diag 20} \end{array} \quad (\text{A.7})$$

and observe that such a half-arc will ‘propagate’ and ultimately lead to a vertical identity diagram \mathbf{I} . This is possible for a right- or left-moving half-arc. Taking the coefficients $-\sin^2 u$ (in the right-moving scenario (A.6)) and $\cos^2 u$ (in the left-moving scenario (A.7)) into consideration, this immediately gives the term proportional to \mathbf{I} in (4.5). Having accounted for all situations with a half-arc, we are left with the two weighted connectivities

$$-\cos u \sin u \begin{array}{c} \text{diag 21} \\ \text{diag 22} \end{array} \quad \text{and} \quad \cos u \sin u \begin{array}{c} \text{diag 23} \\ \text{diag 24} \end{array} \quad (\text{A.8})$$

for each of the N 3-tangles in (A.5). Adding up all possible combinations of these connectivities readily produces the term proportional to \mathbf{J} in (4.5). \square

A.2 Proof of Drop-Down Lemma

Proof of Drop-Down Lemma (Section 4.2) Since a non-trivial arc-part only appears for $N \geq 2$, we assume $N \geq 2$ and consider a segment of \mathbf{J} consisting of two 3-tangles (4.1) with a half-arc linking the two nodes on the upper edge

$$\begin{array}{c} \text{diag 25} \\ \text{diag 26} \end{array} = \begin{array}{c} \text{diag 27} \\ \text{diag 28} \end{array} - \begin{array}{c} \text{diag 29} \\ \text{diag 30} \end{array} - \begin{array}{c} \text{diag 31} \\ \text{diag 32} \end{array} + \begin{array}{c} \text{diag 33} \\ \text{diag 34} \end{array} \quad (\text{A.9})$$

The third diagram of the right side vanishes due to the contractible loop. For $N = 2$, the identification of the left and right vertical edges gives back a half-arc multiplied by $2 - \alpha^2$, and the proof is complete. For $N > 2$, we include the 3-tangle to the left or right, respectively, of the first and fourth diagrams

$$\begin{array}{c} \text{diag 35} \\ \text{diag 36} \end{array} = \begin{array}{c} \text{diag 37} \\ \text{diag 38} \end{array} - \begin{array}{c} \text{diag 39} \\ \text{diag 40} \end{array} = 0 \quad (\text{A.10})$$

$$\begin{array}{c} \text{diag 41} \\ \text{diag 42} \end{array} = \begin{array}{c} \text{diag 43} \\ \text{diag 44} \end{array} - \begin{array}{c} \text{diag 45} \\ \text{diag 46} \end{array} = 0 \quad (\text{A.11})$$

It follows that, for $N > 2$, we simply have

(A.12)

implying that a single half-arc drops down leaving behind a couple of horizontal links (indicated by wavy links in (A.12)) between the two vertical edges. For given arc-part of the input link state, this procedure is repeated starting with the innermost half-arc(s) and working out, as illustrated here

(A.13)

in an example for $N = 12$. \square

A.3 Proof of Sector Lemma

Proof of Sector Lemma (Section 4.2) The lemma is readily verified for $N = 1$. For $N = 2$, there are two link states with $\ell = 0$ and one link state with $\ell = 2$. $\mathbf{J}_0 = \Omega^2 + \Omega^{-2}$ acts as twice the identity. \mathbf{J}_1 maps the link state with $\ell = 2$ into minus the sum of the link states with $\ell = 0$ (which is outside the sector and therefore set to zero), while it maps both link states with $\ell = 0$ into themselves multiplied by $-\alpha^2$. This completes the proof for $N = 2$. For $N > 2$ and $\ell > 0$, we get a factor of $(-1)^{\frac{N-\ell}{2}}$ from the drop-down process. Within the given sector, the ℓ defects are mapped into ℓ defects. This requires the 3-tangles not affected by the drop-down process (as the 9th and 12th 3-tangles in the last diagram of (A.13)) to be identical thereby giving rise to an additional factor of $((-1)^\ell + 1)$. Since this factor is 2 for N, ℓ even and vanishes for N, ℓ odd, we immediately recognize (4.7). Finally, for $N > 2$ and $\ell = 0$, we perform the drop-down process for all but the final, outmost half-arc. This gives a factor of $(-1)^{\frac{N-2}{2}}$ and we are left with a scenario as in (A.9) giving rise to an additional factor of $2 - \alpha^2$. \square

A.4 Matrix \mathbf{J} for an arbitrary number of defects

Here, we continue the description at the end of Section 4.2 of the matrix realization of \mathbf{J} appearing in the Inversion Identity (A.5) for given N when an arbitrary number of defects

is allowed.

To simplify the description, let us introduce the following algebraic abbreviations

$$u = - \begin{array}{|c|} \hline \text{---} \\ \hline \text{---} \\ \hline \text{---} \\ \hline \end{array} , \quad d = \begin{array}{|c|} \hline \text{---} \\ \hline \text{---} \\ \hline \text{---} \\ \hline \end{array} \quad (\text{A.14})$$

allowing us to write a horizontal concatenation of such 3-tangles simply as products of u 's and d 's. For example, ignoring the half-arc linking the nodes on the upper edge in (A.9), the sum of diagrams on the right side of (A.9) reads $uu + ud + du + dd$.

For a link state A , we let $\ell(A)$ denote the number of defects, $\text{arc}(A)$ the arc-part, and $h(A)$ the maximal height of the arcs, where the height of an arc is the maximal number of points of intersection of arcs (on or below the arc itself) with a vertical line through the horizontal line segment between the two end-nodes of the arc. In the first diagram in (A.13), there are thus three arcs of height 1, one arc of height 2, and one arc of height 3.

Letting A and A' denote an input and an output link state, respectively, the corresponding entry of \mathbf{J} is denoted by $\mathbf{J}_{A',A}$. We immediately see that $\mathbf{J}_{A',A} = 0$ if $\ell(A) < \ell(A')$ since defects cannot be created by the action of \mathbf{J} . Furthermore, the blocks with $\ell(A) = \ell(A')$ appearing on the diagonal of \mathbf{J} are themselves diagonal and given by the Sector Lemma (4.7). To complete the description of the matrix realization of \mathbf{J} , we therefore turn to the cases where $\ell(A) > \ell(A')$. The Drop-Down Lemma implies that $\text{arc}(A) \subset \text{arc}(A')$, which we will assume in the following. As discussed in Section 4.2, the data remaining to characterize the matrix \mathbf{J} can be extracted by examining the input link state A_ℓ , for which $\ell(A_\ell) = \ell$ and $\text{arc}(A_\ell) = \emptyset$, for each of the corresponding system sizes $N_\ell = \ell$ where $\ell = N \bmod 2$.

We let A'_ℓ denote an output state resulting when \mathbf{J} acts on A_ℓ . Since A_ℓ consists of defects only, all arcs in A'_ℓ are created by \mathbf{J} . This yields three cases distinguished by the height of A'_ℓ which can take on the values $h(A'_\ell) = 0, 1, 2$ since $\mathbf{J}_{A'_\ell, A_\ell} = 0$ if $h(A'_\ell) > 2$.

For $h(A'_\ell) = 0$, we see that $A'_\ell = A_\ell$ and $\mathbf{J}_{A'_\ell, A_\ell} = (-1)^\ell + 1$.

For $h(A'_\ell) = 1$, we initially assume that $\ell(A'_\ell) = 0$. This presupposes ℓ even, and we readily see that $\mathbf{J}_{A'_\ell, A_\ell} = (-1)^{\frac{\ell}{2}} \alpha$. For given A'_ℓ with $\ell(A'_\ell) > 0$, on the other hand, the contributing terms in the expansion of \mathbf{J} have a specified distribution of 4-tangles ud

$$\dots g_{k_n}^{(n)}(ud)g_1^{(1)} \dots g_{k_1}^{(1)}(ud)g_1^{(2)} \dots g_{k_2}^{(2)}(ud)g_1^{(3)} \dots \quad (\text{A.15})$$

where every g is a u or a d , and where

$$\ell = \ell' + 2n, \quad \sum_{j=1}^n k_j = \ell' \quad (\text{A.16})$$

Since $\ell(A'_\ell) > 0$, there is at least one segment between two neighbouring ud 's (which can be the same ud due to the cylinder topology) in which a u is not followed by a d , that is, $n > 0$. With reference to (A.15), let us assume that this segment is the one indicated by $g_1^{(1)} \dots g_{k_1}^{(1)}$. If $g_{k_1}^{(1)} = u$, we see that $g_1^{(2)} = u$ ($g_1^{(1)} = u$ for $n = 1$) in order to prevent $h(A'_\ell) = 2$. In order to preserve the specified distribution of (ud) 's, every $g_i^{(2)}$ in this segment must be a u . Continuing this argument around the cylinder, implies that all the g 's must be u 's. If, instead, $g_{k_1}^{(1)} = d$, this 3-tangle could be followed, on the other side of the (ud) to its right, by a g being a u . However, this u would force every g to its right to be a u , leading to an

inconsistency with $g_{\kappa_1}^{(1)} = d$ once the cycle has been traversed. We thus conclude that all g 's must be u 's or all g 's must be d 's, implying that $\mathbf{J}_{A'_\ell, A_\ell} = (-1)^{\frac{\ell(A_\ell) - \ell(A'_\ell)}{2}} ((-1)^\ell + 1)$.

For $h(A'_\ell) = 2$, there is at least one arc of height 2. In the contributing terms in the expansion of \mathbf{J} , the 3-tangle containing the leftmost node of this arc must correspond to a u followed by a u to its immediate right, while the 3-tangle containing the rightmost node corresponds to a d preceded by a d to its immediate left, that is,

$$\dots f_{\kappa_\nu}^{(n)}(uu \dots dd) f_1^{(1)} \dots f_{\kappa_1}^{(1)}(uu \dots dd) f_1^{(2)} \dots f_{\kappa_2}^{(2)}(uu \dots dd) f_1^{(3)} \dots \quad (\text{A.17})$$

where every f is a u or a d , while $\kappa_j, \nu \geq 0$. For $\nu = 0$, which presupposes ℓ even, there is only one contributing term, and we see that $\mathbf{J}_{A'_\ell, A_\ell} = (-1)^{\frac{\ell}{2}}$. For $\nu > 0$, every segment $ddf_1^{(j)} \dots f_{\kappa_1}^{(j)}uu$ expands as

$$ddg_1^{(j,1)} \dots g_{\kappa_1}^{(j,1)}(ud)g_1^{(j,2)} \dots g_{\kappa_2}^{(j,2)} \dots (ud)g_1^{(j,n)} \dots g_{\kappa_n}^{(j,n)}uu \quad (\text{A.18})$$

where $k_i, n \geq 0$. As in the argument for $h(A'_\ell) = 1$, a $g = u$ in (A.18) cannot be followed by a $g = d$ in (A.18). Ignoring the 4-tangles (ud) , the sequence of g 's in (A.18) can therefore be any of the $\kappa_j + 1$ sequences of the form $d \dots du \dots u$. Adding up these contributions, while taking into account the 'boundary effects' coming from the sandwiching by $dd \dots uu$ in (A.18), we see that all but one of the terms cancel out pairwise leaving

$$\frac{1 + (-1)^{\kappa_j}}{2} dd(d \dots d(ud)d \dots d \dots (ud)d \dots d)uu \quad (\text{A.19})$$

For $\nu > 0$, the 'value' for $f_{\kappa_j}^{(j)}$ (that is, u or d) does not affect the value for $f_1^{(j+1)}$ ($f_1^{(1)}$ for $j = \nu = 1$). This independence of the segments implies that $\mathbf{J}_{A'_\ell, A_\ell}$ is given by the product of the ν contributions just obtained (being 0 or 1)

$$\mathbf{J}_{A'_\ell, A_\ell} = \begin{cases} 0, & \text{if any } \kappa_j \text{ is odd} \\ 1, & \text{if all } \kappa_j \text{ are even} \end{cases} \quad (\text{A.20})$$

In summary, $\mathbf{J} = 0$ for N odd, while, for N even, \mathbf{J} is a sparse upper-triangular matrix whose non-vanishing entries are given by

$$\mathbf{J}_{A', A} = (-1)^{\frac{N - \ell'}{2}} \begin{cases} 2 + (\alpha^2 - 4)\delta_{\ell', 0}, & \text{if } A' = A \\ 2 + (\alpha - 2)\delta_{\ell', 0}, & \text{if } h_{A', A} = 1 \\ 1, & \text{if } h_{A', A} = 2, s_{A', A} \subset 2\mathbb{N}_0 \end{cases} \quad (\text{A.21})$$

where $\ell' = \ell(A')$ and $h_{A', A} = h(\text{arc}(A') \setminus \text{arc}(A))$, while $s_{A', A}$ is the set of numbers of nodes between the rightmost node of a height-2 arc of $\text{arc}(A') \setminus \text{arc}(A)$ and the leftmost node of the next height-2 arc to its right (which, due to the cylinder topology, can be the same height-2 arc). It is noted, that $h_{A', A} = 1, 2$ requires that $\text{arc}(A) \subsetneq \text{arc}(A')$.

For N even, we observe that the sum of the entries of a column of \mathbf{J} is given by

$$C = (-1)^{\frac{N}{2}} \begin{cases} \alpha^2 - 2, & \ell = 0 \\ 2\alpha - 2, & \ell = 2 \pmod{N} \end{cases} \quad (\text{A.22})$$

For given N , these sums are all equal if and only if $\alpha = 0, 2$.

References

- [1] P. Flory, *Statistical mechanics of chain molecules*, Interscience (1969);
P.G. de Gennes, *Exponents for the excluded volume problem as derived by the Wilson method*, Phys. Lett. **A38** (1972) 339–340; *Scaling Concepts in Polymer Physics*, Cornell University, Ithaca (1979);
J. des Cloizeaux, *The Lagrangian theory of polymer solutions at intermediate concentrations*, J. Phys. (Paris) **36** (1975) 281–291.
- [2] H. Saleur, *New exact exponents for the two-dimensional self-avoiding walks*, J. Phys. **A19** (1986) L807–L810; *Conformal invariance for polymers and percolation*, J. Phys. **A20** (1987) 455–470; *Magnetic properties of the two-dimensional $n = 0$ vector model*, Phys. Rev. **B35** (1987) 3657–3660.
- [3] B. Duplantier, *Exact critical exponents for two-dimensional dense polymers*, J. Phys. **A19** (1986) L1009–L1014.
- [4] H. Saleur, *Polymers and percolation in two dimensions and twisted $N = 2$ supersymmetry*, Nucl. Phys. **B382** (1992) 486–531, arXiv:hep-th/9111007.
- [5] V. Gurarie, *Logarithmic operators in conformal field theory*, Nucl. Phys. **B410** (1993) 535–549, arXiv:hep-th/9303160.
- [6] P.A. Pearce, J. Rasmussen, J.-B. Zuber, *Logarithmic minimal models*, J. Stat. Mech. **0611** (2006) P017, arXiv:hep-th/0607232.
- [7] N. Read, H. Saleur, *Associative-algebraic approach to logarithmic conformal field theories*, Nucl. Phys. **B777** (2007) 316–351, arXiv:hep-th/0701117.
- [8] P.A. Pearce, J. Rasmussen, *Solvable critical dense polymers*, J. Stat. Mech. **0702** (2007) P015, arXiv:hep-th/0610273.
- [9] A. Nigro, *Integrals of motion for critical dense polymers and symplectic fermions*, J. Stat. Mech. **0910** (2009) P007, arXiv:0903.5051 [hep-th]; *The Baxter Q operator of critical dense polymers*, J. Stat. Mech. **0910** (2009) P008, arXiv:0905.0285 [hep-th].
- [10] V.F.R. Jones, *A quotient of the affine Hecke algebra in the Brauer algebra*, L’Enseignement Math. **40** (1994) 313–344; *Planar algebras I*, arXiv:math.QA/9909027.
- [11] H.N.V. Temperley, E.H. Lieb, *Relations between the ‘percolation’ and ‘colouring’ problem and other graph-theoretical problems associated with regular planar lattices: some exact results for the ‘percolation’ problem*, Proc. Roy. Soc. Lond. **A322** (1971) 251–280;
V. Pasquier, H. Saleur, *Common structures between finite systems and conformal field theories through quantum groups*, Nucl. Phys. **B330** (1990) 523–556;
P.P. Martin, *Potts models and related problems in statistical mechanics*, Series on Advances in Statistical Mechanics, Volume 5, World Scientific, Singapore (1991);
P.P. Martin, H. Saleur, *On an algebraic approach to higher dimensional statistical mechanics*, Commun. Math. Phys. **158** (1993) 155–190, arXiv:hep-th/9208061; *The blob algebra and the periodic Temperley-Lieb algebra*, Lett. Math. Phys. **30** (1994) 189–206, arXiv:hep-th/9302094.

- [12] N. Read, H. Saleur, *Exact spectra of conformal supersymmetric nonlinear sigma models in two dimensions*, Nucl. Phys. **B613** (2001) 409–444, arXiv:hep-th/0106124.
- [13] R.J. Baxter, *Exactly solved models in statistical mechanics* (London, 1982) Academic Press, particularly Section 7.7.
- [14] P.A. Pearce, J. Rasmussen, P. Ruelle, *Integrable boundary conditions and \mathcal{W} -extended fusion in the logarithmic minimal models $\mathcal{LM}(1,p)$* , J. Phys. **A41** (2008) 295201, arXiv:0803.0785 [hep-th].
- [15] H.G. Kausch, *Symplectic fermions*, Nucl. Phys. **B583** (2000) 513–541, arXiv:hep-th/0003029.
- [16] M.A.I. Flohr, *On modular invariant partition functions of conformal field theories with logarithmic operators*, Int. J. Mod. Phys. **A11** (1996) 4147–4172, arXiv:hep-th/9509166; M.R. Gaberdiel, H.G. Kausch, *A rational logarithmic conformal field theory*, Phys. Lett. **B386** (1996) 131–137, arXiv:hep-th/9606050; M.R. Gaberdiel, I. Runkel, *From boundary to bulk in logarithmic CFT*, J. Phys. A: Math. Theor. **41** (2008) 075402, arXiv:0707.0388 [hep-th].
- [17] P.A. Pearce, V. Rittenberg, J. de Gier, B. Nienhuis, *Temperley-Lieb stochastic processes*, J. Phys. **A35** (2002) L661–L668, arXiv:math-ph/0209017.
- [18] E. Melzer, *Fermionic character sums and the corner transfer matrix*, Int. J. Mod. Phys. **A9** (1994) 1115–1136, arXiv:hep-th/9312043; A. Berkovich, *Fermionic counting of RSOS-states and Virasoro character formulas for the unitary minimal series $M(\mu, \mu + 1)$. Exact results*, Nucl. Phys. **B431** (1994) 315–348 arXiv:hep-th/9403073.
- [19] D. Levy, *Algebraic structure of translation-invariant spin-1/2 xxz and q -Potts quantum chains*, Phys. Rev. Lett. **67** (1991) 1971–1974.
- [20] L.H. Kauffman, *State models and the Jones polynomial*, Topology **26** (1987) 395–407.
- [21] D.L. O’Brien, P.A. Pearce, S.O. Warnaar, *Finitized conformal spectrum of the Ising model on the cylinder and torus*, Physica **A228** (1996) 63–77.
- [22] H.W.J. Blöte, J.L. Cardy, M.P. Nightingale, *Conformal invariance, the central charge, and universal finite-size amplitudes at criticality*, Phys. Rev. Lett. **56** (1986) 742–745.
- [23] I. Affleck, *Universal term in the free energy at a critical point and the conformal anomaly*, Phys. Rev. Lett. **56** (1986) 746–748.
- [24] M. Abramowitz, I.A. Stegun, *Handbook of mathematical functions*, National Bureau of Standards Applied Mathematics Series - 55 (1964).
- [25] P.A. Pearce, J. Rasmussen, *Physical combinatorics of critical dense polymers*, in preparation (2010).
- [26] J. Fürlinger, J. Hofbauer, *q -Catalan numbers*, J. Combin. Theory **A40** (1985) 248–264; P. Brändén, *q -Narayana numbers and the flag h -vector of $J(2 \times N)$* , Discrete Math. **281** (2004) 67–81, arXiv:math/0211318.